Journal of Sound and Vibration (1998) **209**(5), 723–752

A FIRST ORDER SYSTEM SOLUTION FOR THE VECTOR WAVE EQUATION IN A RESTRICTED CLASS OF HETEROGENEOUS MEDIA

G. D. MANOLIS

Department of Civil Engineering, *Aristotle University*, *Thessaloniki* 54006, *Greece*

R. P. SHAW

Department of Civil Engineering, *State University of New York*, *Buffalo*, *New York* 14260, *U.S.A.*

AND

S. PAVLOU

Department of Chemical Engineering, *University of Patras*, *Patras* 26500, *Greece*

(*Received* 27 *January* 1997, *and in final form* 30 *June* 1997)

A fundamental solution is derived for time harmonic elastic waves originating from a point source and propagating in a restricted class of three-dimensional, unbounded heterogeneous media which have a Poisson ratio of 0·25 and elastic moduli that vary quadratically with respect to the depth co-ordinate. The first step in the solution procedure is to transform the displacement vector in the equations of dynamic equilibrium through scaling by the square root of the position-dependent shear modulus. The constraints generated through this procedure are satisfied by quadratic (in the depth co-ordinate) profiles of the elastic moduli. During the next step, a double Fourier transform with respect to the horizontal co-ordinates is applied to the dynamic equilibrium equations, which assume a form amenable to solution by a first order matrix differential equation system. This latter system is solved using a series expansion due to the presence of non-constant matrix coefficients. The last step in recovering the fundamental solution is inversion of the double Fourier transform. This is accomplished numerically through use of the FFT, because complexity of the first order system approach precludes analytic inversion. Finally, some numerical examples serve to illustrate the present methodology.

1. INTRODUCTION

Wave propagation through naturally occurring and man-made materials is of interest in view of widespread applications in acoustic and electromagnetic signal transmissions, seismically induced motions, non-destructive testing evaluation, noise control, subsurface exploration, etc. [1–4]. Due to the complex structure of such media, wave propagation is invariably accompanied by reflection, refraction, diffraction and scattering phenomena that are difficult to quantify. Elastic waves in discretely layered media and in variable velocity layers are discussed in Ewing *et al*. [1] and in Ben-Menachem and Singh [2], where the basic problem of inseparability of waves into dilatational and rotational components (unless the variation of the material parameters is small compared to the wavelength) is brought forth. Brekhovskikh and Beyer [3] and Chew [4] examine primarily acoustic and electromagnetic waves, with the former reference focusing on wave reflection and refraction in discrete as well as in continuously layered media and the latter on specialized

0022–460X/98/050723 + 30 $25.00/0/sv971333

methods (e.g., Green functions, integral equations, the T-matrix approach, etc.), which can be used for numerical solution of problems involving waves in planarly, cylindrically and spherically layered media. In general, most of the work on waves in inhomogeneous continua focuses on acoustic and electromagnetic waves in discretely layered media and under time harmonic conditions. Of major importance is the scalar wave equation with a depth-dependent wavenumber, because it corresponds to (i) sound waves in which the acoustic medium density variation over the wavelength is important, (ii) electromagnetic waves in which the electric field is polarized and (iii) horizontally (SH) and vertically (SV) polarized elastic shear waves. In the case of SV waves, it is necessary to resort to a potential representation of the displacement vector in order to recover two scalar wave equations, so certain restrictions on the degree of medium inhomogeneity need to be imposed.

Various methodologies are available for solving scalar waves in inhomogeneous media [3–8]. One class of specialized analysis techniques is based on geometrical optics approximation for high frequencies and large wavenumbers. The applicability of geometrical optics hinges on the fact that, at high frequencies, we have small values of the corresponding wavelength and the effect of inhomogeneities on the propagating wave is considerably diminished. For problems involving wave propagation in discretely layered media, a layer is subdivided into several sublayers, so as to obtain a good description of the displacement field, and the accuracy of the representation is conditional upon the frequency of excitation. For media in which the dependence of their material parameters on position is arbitrary, a different class of techniques based on successive approximations is available. Although the wave field in arbitrary inhomogeneous media can be represented in terms of position-dependent amplitude and phase angle, it is not possible uniquely to divide it into the sum of incident plus reflected waves due to continuous scattering of the signal by the inhomogeneities. Also, the need to account for the presence of a source in the continuum generates some new problems. In the case of discretely layered inhomogeneous media, the method of images is often used as a way of reproducing the correct boundary conditions at the interface directly below or above the source. In the case of continuously inhomogeneous media, the ray theory of waveguide propagation is used as a high frequency approximation and for distances between source and receiver that are not large.

There are relatively few closed form solutions available in the literature for waves in layered media due to point sources (Green functions). One of the earliest derivations was by Pekeris [9] for a half-space in which the refractive index variation is inversely proportional to the depth co-ordinate. As far as the heterogeneous Helmholtz equation governing propagation of time harmonic acoustic or horizontally polarized elastic shear waves is concerned, we have the work of Li *et al*. [10], who presented an exact analytic solution for a point source in a three-dimensional medium with a refractive index in the form of the square root of a simple polynomial in the depth co-ordinate. Approximate solutions can also be generated, e.g., by decomposing the inhomogeneous medium into a stack of laterally varying layers and representing the solution within a layer as a sum of decoupled plane waves [11]. A very general numerical technique for investigating seismic wave propagation in anisotropic, porous or viscoelastic materials is presented in the review paper by Mikhailenko [12]. In particular, different families of algorithms are suggested based on a combination of finite integral transforms with finite difference techniques for the computation of complete seismograms in complex, three-dimensional subsurface geometries. Of interest here are (a) the inhomogeneous isotropic 3-D medium in which the elastic parameters and the density are functions of depth [12] and (b) SH wave propagation in a heterogeneous medium in which the wavespeed is a function of two spatial variables [13]. In the former case, the equations of motion are described in cylindrical co-ordinates

and the method of approach is a double Hankel integral transformation with respect to the two spatial variables, followed by a finite difference solution and inverse transformations. The latter case combines a finite Fourier integral transformation in one spatial co-ordinate with a finite difference scheme in the other co-ordinate. All spatial derivatives encountered in the finite difference method are approximated by Fourier series [14] for better accuracy.

As previously mentioned, an effective method for investigating wave propagation in a continuously layered medium is to employ a Fourier–Bessel transformation so as to obtain an integral representation of the wavefield. Evaluation of these integral expressions requires integration over the complex plane and the contributions coming from the poles are known as normal modes. Each normal mode satisfies the wave equation and propagates with its own velocity. Applications of this method include scalar wave propagation in a layer with a wavenumber that depends linearly on depth and in an Epstein layer. A complete list of known solutions for reflection of scalar waves in inhomogeneous layers appears in Brekhovskikh and Beyer [3], and includes wavenumbers that vary with depth as the power of a linear function, as the inverse of a linear function, as general polynomials that start from the second power onwards and as the exponential function. For wave fields that exhibit cylindrical symmetry, three potentials corresponding to P, SV and SH can then be defined. The SH wave case is completely equivalent to an acoustic problem, while the P and SV cases remain coupled. Another method for determining the wavefield due to a point source in an inhomogeneous medium satisfying certain conditions (such as constant density or a Poisson ratio of 0·25 or a linear wavespeed gradient) which allow for independent P and S equations of motion is developed in Acharya [15]. By assuming cylindrical symmetry and representing the pulse from the point source as a superposition of harmonic waves, the total field is obtained by summing over all plane waves and then integrating the sum over all values of the direction cosines. Thus, integral expressions are obtained for the compressional and shear potentials that are convergent. In the case in which the material parameters of the medium are functions of more than one co-ordinate, then the properties of the waveguide change along its direction of propagation. This case is known as the inhomogeneous waveguide and a few approximate techniques have been devised for these problems, such as finding the high frequency asymptote and the method of transverse cross-sections for low frequency solutions. Applications include plane problems with the wave speed being a function of two co-ordinates [3] and ray formulation for the wavespeed being a function of three co-ordinates [16].

Other early analytical work addressing wave motions in non-homogeneous media is by Hook [17], on the method of separation of variables in order to recast the vector wave equation with position-dependent material parameters into a system of three linearly independent solutions for the corresponding number of scalar potentials, which in turn satisfy second order wave equations. This can always be achieved for SH waves, while formulations for SV and P wave are possible only for certain functional forms of the mechanical properties, such as power laws for the shear modulus and density and a fixed value of Poisson ratio. Furthermore, the wave equations for the latter two potentials are coupled, implying that P and SV waves are no longer purely dilatational and rotational. It therefore becomes necessary to impose further constraints on the material parameters in order to achieve two uncoupled P and SV wave equations. This approach was generalized in a later publication [18] though introduction of a linear transformation for the displacement vector in order to produce a diagonal system matrix for the vector wave equation, which was reformulated by using matrix notation. The method of separation of variables for non-homogeneous media was implemented for the axisymmetric case (with plane strain being a special case) and the resulting constraints which dictate mathematically

acceptable material parameter variations with respect to a single spatial co-ordinate appear in the form non-linear ordinary differential equations. Other work along the lines of separation of the displacement vector in a non-homogeneous medium into P and S wave potentials is by Gupta [19], who obtained reflection coefficients for a layer (in which the elastic parameters are quadratic functions of the depth co-ordinate and the Poisson ratio is equal to 0·25) sandwiched between two elastic, homogeneous halfspaces. Furthermore, Payton [20] solved the uni-dimensional wave equation for a pulse travelling in a composite rod exhibiting a constant wavespeed on one part and a quadratically varying one on the other part by using the Laplace transform technique. Finally, a general technique for solving the vector wave equation in an arbitrary non-homogeneous medium is by Karal and Keller [21], who introduced an expansion of the solution in terms of asymptotic series. This technique does not require separability in the sense previously discussed, but the calculations required in order to obtain successive terms of the series are extremely tedious.

Also of interest is the generation of synthetic signals in layered media due to various point sources. For instance, a computationally stable solution for determining surface displacements due to buried dislocation sources in a multi-layered elastic medium was developed by Wang and Herrmann [22] based on the work of Haskell [23], who employed the Fourier transformation and evaluated signal time histories for the elastic medium by performing contour integration of Bessel functions in the complex wavenumber plane. In general, solution procedures for seismic wave motions due to buried sources follow along two lines; namely, Laplace transform or Cagniard–de Hoop technique [24] and Fourier transform [25]. The former technique is also known as generalized ray method because the solution is constructed by tracking the individual seismic signal arrivals ray by ray from source to receiver. It is valid at high frequencies, but not well suited for cases with many layers and large source to receiver distances. In the latter technique, the complete wave solution is expressed in terms of double integral transformations over wavenumber and frequency. The method can handle a large number of plane layers, but requires considerable computational effort at high frequencies. It is also possible to introduce numerical techniques for carrying out the contour integrations [26]. A comprehensive work on the three-dimensional response of a viscoelastic layered half-space to a buried source is that of Apsel and Luco [27], who performed careful comparisons between their technique, which is based on numerical evaluation of a Hankel-type integral using the contour integration method, with analytical solutions, finite elements, the discrete wavenumber formulation and with the generalized ray method. Furthermore, an often used concept is that of transfer matrices, which was pioneered in the field of seismology by Thomson [28]. Transfer matrices relay information (forces and displacements) between upper and lower interfaces of an individual layer and can be used to approximate continuously heterogeneous media as well. Furthermore, they may be synthesized as finite elements to model multi-layered structure [29] and can be extended to wave amplification problems in two-dimensional deposits [30].

The purpose of this work is to address elastic wave propagation in a three-dimensional, unbounded heterogeneous medium. However, due to the inherent complexity of such a problem, heterogeneity is restricted to a depth-only dependence of the material parameters, which correspond to a Poisson ratio of 0·25 and which combine in such a way that linear or square root of a linear function wavespeed profiles are produced. More specifically, this paper is structured as follows. First, the governing equations of motion in an unbounded heterogeneous medium in which material properties vary arbitrarily with position are presented. Next, an algebraic transformation is applied to the displacement vector through which the equilibrium equations attain a form that no longer involves derivatives of the material parameters. This process generates a number of constraint equations, which

dictate a Poisson ratio of 0·25 and a quadratic variation with respect to the depth coordinate of the elastic moduli. Subsequently, a double Fourier transform is applied to the equilibrium equations, which are recast as a first order, matrix differential equation system. Finally, a fundamental solution (Green functions) due to a point impulse is obtained through a series expansion solution of the matrix equation system followed by inversion using the double fast Fourier transform (FFT). Since the above derivation is for time harmonic conditions, viscoelastic material behavior can be introduced through use of complex representations of the elastic moduli. The present methodology is based, to a certain extent, on earlier work using algebraic transformations [31] and first order differential equation system solutions [32] for wave propagation problems. The fundamental solution obtained herein is numerically evaluated for density profiles which are polynomials in the depth co-ordinate and some results are given for both steady state and transient conditions.

2. GOVERNING EQUATIONS OF MOTION FOR A HETEROGENEOUS MEDIUM

In a linear elastic, isotropic medium the dynamic equilibrium equations, the kinematic relations and the constitutive law are [33]

$$\sigma_{ij,j} + \varrho f_i = \varrho \ddot{u}_i, \qquad \varepsilon_{ij} = \tfrac{1}{2}(u_{i,j} + u_{j,i}), \qquad \sigma_{ij} = \lambda\theta\delta_{ij} + 2\mu\varepsilon_{ij}, \tag{1}$$

respectively. In the above, u_i, ϱf_i, ε_{ij} and σ_{ij} respectively are displacements, body force per unit volume, strain and stress, while λ and μ are the Lamé elastic constants and ϱ is the density. Furthermore,

$$\theta = \varepsilon_{kk} = u_{k,k} \tag{2}$$

is the dilatation. All indices range from 1 to 3, with commas indicating partial differentiation with respect to the spatial co-ordinates x_i and dots indicating partial derivatives with respect to time t. Finally, the summation convention is implied for repeated indices and δ_{ij} is Kronecker's delta.

In the case of a homogeneous medium, equations (1) and (2) can be combined to give the displacement equations that govern elastic wave motion, as

$$(\lambda + \mu)u_{j,ji} + \mu u_{i,jj} + \varrho f_i = \varrho \ddot{u}_i \tag{3}$$

or, in vector form, as

$$(\lambda + \mu)\nabla\nabla \cdot \mathbf{u} + \mu\nabla^2\mathbf{u} + \varrho\mathbf{f} = \varrho\ddot{\mathbf{u}}, \tag{4}$$

where ∇ is the gradient and $\nabla^2 = \nabla \cdot \nabla$ is the Laplacian.

If the continuum is heterogeneous (see Figure 1), then the material parameters are position dependent (e.g., $\lambda = \lambda(\mathbf{x})$, $\mu = \mu(\mathbf{x})$, $\varrho = \varrho(\mathbf{x})$) and the equations of motion are recovered in a form different from that shown above. More specifically, equations (1) combine to give the governing equation of motion in the form

$$\{\lambda(\mathbf{x})u_{k,k}(\mathbf{x}, t)\}_{,i} + \{\mu(\mathbf{x})(u_{i,j}(\mathbf{x}, t) + u_{j,i}(\mathbf{x}, t))\}_{,j} + \varrho(\mathbf{x})f_i(\mathbf{x}, t) = \varrho(\mathbf{x})\ddot{u}_i(\mathbf{x}, t) \tag{5}$$

Once the differentiations have been carried out one has, in vector form,

$$\nabla\{(\lambda + 2\mu)\theta\} + \mu\nabla^2\mathbf{u} - \mu\nabla\theta - 2\theta\nabla\mu + 2\nabla\mu \cdot \underline{E} + \varrho\mathbf{f} = \varrho\ddot{\mathbf{u}}, \tag{6}$$

where $\underline{E}$ is the strain tensor ε_{ij}. The above equation appears in Ewing *et al*. [1], where it is mentioned that unless the variation of the material parameters over a wavelength is small, there is coupling between pressure and shear waves at every point of the medium.

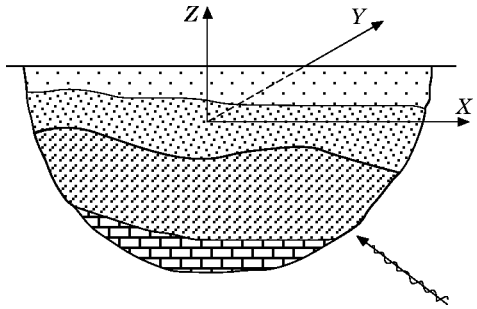

Figure 1. A non-homogeneous medium with depth-dependent material properties.

Therefore, an approach based on the Helmholtz vector decomposition [33] will not work, which is easy to verify.

2.1. THE GREEN FUNCTION FOR HOMOGENEOUS MATERIALS

The Green function solution of equation (3) for a point force f_i of magnitude f at source $\boldsymbol{\xi}$ and under time harmonic conditions is [33]

$$g_{ij}^{h}(r,\omega)=\frac{f}{4\pi\omega^2 r}\left[\exp(\mathrm{i}k_p r)\{\alpha\}-\exp(\mathrm{i}k_s r)\{\beta\}\right], \tag{7}$$

with

$$\{\alpha\}=\mathrm{i}k_p\left\{\mathrm{i}k_p\frac{x_i x_j}{r^2}+\frac{\delta_{ij}}{r}-3\frac{x_i x_j}{r^3}\right\}-\frac{\delta_{ij}}{r^2}+3\frac{x_i x_j}{r^4},$$

$$\{\beta\}=\mathrm{i}k_s\left\{\mathrm{i}k_s\left(\frac{x_i x_j}{r^2}+\delta_{ij}\right)+\frac{\delta_{ij}}{r}-3\frac{x_i x_j}{r^3}\right\}-\frac{\delta_{ij}}{r^2}+\frac{3x_i x_j}{r^4}, \tag{8}$$

where the wavenumbers $k_p=\omega/c_p$ and $k_s=\omega/c_s$. In the above, x_i are co-ordinates of the receiver $\mathbf{x}$ at which the displacement components g_{ij}^{h} are registered, assuming that source $\boldsymbol{\xi}$ is at the origin, and r is the radial distance between them. Furthermore, c_p and c_s respectively are wavespeeds of the pressure (P) and shear (S) waves in the homogeneous continuum, while ω is the frequency of vibration.

3. ALGEBRAIC TRANSFORMATION PROCEDURE

In order to obtain a fundamental solution for the dynamic equilibrium equations (5) governing elastic wave propagation in a heterogeneous 3-D continuum, the following transformation [31] is established for the displacement vector $\mathbf{u}=(u_1,u_2,u_3)$:

$$\mathbf{u}(\mathbf{x},t)=T(\mathbf{x})\mathbf{U}(\mathbf{x},t), \tag{9}$$

where the precise form of T has yet to be determined. Using indical notation, the various derivatives of u_i with respect to the spatial co-ordinates are as follows:

$$u_{i,j}=TU_{i,j}+T_{,j}U_i,\qquad u_{i,jj}=TU_{i,jj}+2T_{,j}U_{i,j}+T_{,jj}U_i,$$
$$u_{j,ij}=TU_{j,ij}+T_{,j}U_{j,i}+T_{,i}U_{j,j}+T_{,ij}U_j. \tag{10}$$

Substituting equations (9) and (10) into the equations of dynamic equilibrium and collecting terms yields the following equations in terms of the transformed displacement vector U_i:

$$\begin{aligned}&\{T\lambda + T\mu\}U_{j,ij} + \{T\mu\}U_{i,jj} + \{2\mu T_{,j} + \mu_{,j}\,T\}U_{i,j}\\&\quad+\{\lambda T_{,j} + \mu T_{,j} + \mu_{,j}\,T\}U_{j,i} + \{\lambda T_{,i} + \lambda_{,i}\,T + \mu T_{,i}\}U_{j,j}\\&\quad+\{\lambda T_{,jj} + \mu_{,j}\,T_{,j}\}U_i + \{\lambda T_{,ij} + \lambda_{,i}\,T_{,j} + \mu T_{,ij} + \mu_{,j}\,T_{,i}\}U_j + \varrho f_i = \varrho T\ddot{U}_i.\end{aligned} \tag{11}$$

If transformation T is chosen such that

$$2\mu T_{,j} + \mu_{,j}\,T = 0, \tag{12}$$

then

$$T(\mathbf{x}) = \mu^{-1/2}(\mathbf{x}). \tag{13}$$

The spatial derivatives of T are therefore

$$T_{,i} = -0{\cdot}5\mu^{-3/2}\mu_{,i}, \qquad T_{,ij} = 0{\cdot}75\mu^{-5/2}\mu_{,i}\,\mu_{,j} - 0{\cdot}5\mu^{-3/2}\mu_{,ij}. \tag{14}$$

By substituting the above expressions for T into equation (11), one obtains the following equilibrium equation:

$$\begin{aligned}&\{\mu^{-1/2}(\lambda + \mu)\}U_{j,ij} + \{\mu^{-1/2}\mu\}U_{i,jj}\\&\quad+\{-0{\cdot}5(\lambda + \mu)\mu^{-3/2}\mu_{,j} + \mu^{-1/2}\mu_{,j}\}U_{j,i}\\&\quad+\{-0{\cdot}5(\lambda + \mu)\mu^{-3/2}\mu_{,i} + \mu^{-1/2}\lambda_{,i}\}U_{j,j}\\&\quad+\{\mu(0{\cdot}75\mu^{-5/2}\mu_{,j}\,\mu_{,j} - 0{\cdot}5\mu^{-3/2}\mu_{,jj}) - 0{\cdot}5\mu^{-3/2}\mu_{,j}\,\mu_{,j}\}U_i\\&\quad+\{(\lambda + \mu)\,(0{\cdot}75\mu^{-5/2}\mu_{,i}\,\mu_{,j} - 0{\cdot}5\mu^{-3/2}\mu_{,ij}) - 0{\cdot}5\mu^{-3/2}\mu_{,j}\,(\lambda_{,i} + \mu_{,i})\}U_j\\&\quad+\varrho f_i = \varrho\mu^{-1/2}\ddot{U}_i.\end{aligned} \tag{15}$$

The above can be simplified by removing $\mu^{-1/2}$ as a common factor, to give

$$\begin{aligned}&\{\lambda + \mu\}U_{j,ij} + \mu U_{i,jj}\\&\quad+\left\{-0{\cdot}5\,\frac{\lambda}{\mu}\,\mu_{,j} + 0{\cdot}5\mu_{,j}\right\}U_{j,i} + \left\{-0{\cdot}5\,\frac{\lambda}{\mu}\,\mu_{,i} - 0{\cdot}5\mu_{,i} + \lambda_{,i}\right\}U_{j,j}\\&\quad+\{0{\cdot}25\mu^{-1}\mu_{,j}\,\mu_{,j} - 0{\cdot}5\mu_{,jj}\}U_i\\&\quad+\left\{0{\cdot}75\left(\frac{\lambda}{\mu^2} + \mu^{-1}\right)\mu_{,i}\,\mu_{,j} - 0{\cdot}5\left(\frac{\lambda}{\mu} + 1\right)\mu_{,ij} - \frac{0{\cdot}5}{\mu}\,(\lambda_{,i} + \mu_{,i})\mu_{,j}\right\}U_j + \varrho\mu^{1/2}f_i = \varrho\ddot{U}_i.\end{aligned} \tag{16}$$

In order to remove all terms multiplying the lower order derivatives, the following constraint equations are identified:

$$\left(-0{\cdot}5\,\frac{\lambda}{\mu} + 0{\cdot}5\right)\mu_{,j} = 0, \qquad \left(-0{\cdot}5\,\frac{\lambda}{\mu} - 0{\cdot}5\right)\mu_{,i} + \lambda_{,i} = 0, \qquad \left(0{\cdot}25\,\frac{1}{\mu}\,\mu_{,j}\,\mu_{,j} - 0{\cdot}5\mu_{,jj}\right) = 0,$$

$$0{\cdot}75\left(\frac{\lambda}{\mu^2} + \frac{1}{\mu}\right)\mu_{,i}\,\mu_{,j} - 0{\cdot}5\left(\frac{\lambda}{\mu} + 1\right)\mu_{,ij} - \frac{0{\cdot}5}{\mu}\,(\lambda_{,i} + \mu_{,i})\mu_{,j} = 0. \tag{17}$$

The first constraint equation requires either a constant μ (i.e., the trivial solution) or

$$\lambda = \mu \tag{18}$$

which corresponds to a Poisson ratio of 0·25 (a rather common value for rock materials [2]). The second constraint equation is automatically satisfied if $\lambda = \mu$, while the remaining two are, respectively,

$$0{\cdot}25\mu^{-1}\mu_{,j}\,\mu_{,j} - 0{\cdot}5\mu_{,jj} = 0 \qquad \text{and} \qquad 0{\cdot}25\mu^{-1}\mu_{,i}\,\mu_{,j} - 0{\cdot}5\mu_{,ij} = 0. \tag{19}$$

If material parameters λ and μ (and consequently ϱ) are assumed to be functions of only one spatial co-ordinate (depth $z = x_3$ for convenience), both of equations (19) are equivalent to

$$(\partial\mu(z)/\partial z)^2 - 2\mu(z)\partial^2\mu(z)/\partial z^2 = 0, \tag{20}$$

the solution to which is

$$\mu(z) = (c_0\, z + c_1)^2, \tag{21}$$

where c_0 and c_1 are constants; i.e., we obtain a quadratic profile of the shear modulus with respect to the depth co-ordinate. By taking all the above constraints into account, the final form of the dynamic equilibrium equations is therefore

$$\mu(z)U_{i,jj} + 2\mu(z)U_{j,ij} + \varrho(z)\mu^{1/2}(z)f_i = \varrho(z)\ddot{U}_i. \tag{22}$$

Introducing the transformation of equation (9) for the body force density **f**, i.e.,

$$\mathbf{F}(\mathbf{x}, t) = \mu^{1/2}(z)\mathbf{f}(\mathbf{x}, t) \tag{23}$$

in the dynamic equilibrium equation yields

$$U_{i,jj} + 2U_{j,ij} + \alpha^2(z)F_i = \alpha^2(z)\ddot{U}_i, \tag{24}$$

where

$$\alpha(z) = \sqrt{\varrho(z)/\mu(z)} \tag{25}$$

is the shear wave slowness (inverse of shear wavespeed) in sec/m. At this stage, the usual Helmholtz decomposition of the displacement vector into dilational and rotational components will not work in conjunction with equation (24) due to the presence of the non-constant slowness $\alpha(z)$. In earlier work [31], this ratio was assumed to be constant (which implies a quadratic depth profile for the density) and vector decomposition was applied to obtain a Green function. This procedure, however, results in a rather severe restriction on the variation of the pressure and shear wave speeds. Specifically,

$$c_p = \sqrt{3\mu(z)/\varrho(z)} = \sqrt{3}/\alpha(z) \qquad \text{and} \qquad c_s = \sqrt{\mu(z)/\varrho(z)} = 1/\alpha(z) \tag{26}$$

would be constant due to the proportional variation of all material parameters. Therefore, a different solution path must be sought, as discussed in the next section.

3.1. TIME HARMONIC CONDITIONS

At this stage, we assume time harmonic conditions for both transformed displacement and forcing function vectors in the form

$$U_i(\mathbf{x}, t) = U_i(\mathbf{x})\exp(\mathrm{i}\omega t), \qquad F_i(\mathbf{x}, t) = F_i(\mathbf{x})\exp(\mathrm{i}\omega t), \tag{27}$$

where ω is the frequency of vibration in rad/s. Therefore, the steady state form of the governing equations of motion is

$$U_{i,jj} + 2U_{j,ij} + \alpha^2(z)F_i + \omega^2\alpha^2(z)U_i = 0 \tag{28}$$

and the transient response can be recovered through Fourier synthesis.

4. FIRST ORDER SYSTEM FORMULATION VIA DOUBLE FOURIER TRANSFORMATION

In this section, we apply the Fourier transformation twice with respect to the spatial variables $(x_1, x_2) = (x, y)$ to the dynamic equilibrium equations (28) in order to recover a form which contains derivatives with respect to the z co-ordinate only and, as such, are amenable to a first order differential equation system solution. The particular variant of the exponential Fourier transformation that will be employed here is defined as

$$F(h) = \bar{h}(\omega) = \int_{-\infty}^{\infty} h(t)\exp(\mathrm{i}\omega t)\,\mathrm{d}t,$$

$$F^{-1}(\bar{h}) = h(t) = \frac{1}{2\pi}\int_{-\infty}^{\infty} \bar{h}(\omega)\exp(-\mathrm{i}\omega t)\,\mathrm{d}\omega, \tag{29}$$

where F and F^{-1} respectively are the direct and inverse transforms [34]. We mention the operational property for the nth derivative of function $h(t)$ as

$$F(h^{(n)}) = (-\mathrm{i}\omega)^n\bar{h}(\omega), \tag{30}$$

and the transform of the Dirac delta function $\delta(t)$ (point impulse at time $t = 0$) as

$$F(\delta) = 1{\cdot}0. \tag{31}$$

It is also noted that since the Fourier transformation is defined through both positive and negative time (and frequency) values, no initial conditions are associated with $t = 0$. Finally, $h(t)$ and its derivatives must remain bounded; i.e.,

$$\lim_{|t|\to\infty} |\, h^{(n)}(t)\,| = 0 \qquad (n = 0, 1, 2, \ldots). \tag{32}$$

As previously mentioned, the (t, ω) pair is the standard definition of the Fourier transform. We will employ a double Fourier transform involving the pairs (x, k_1) and (y, k_2), where k_1 and k_2 are wavenumbers in m^{-1}. The notation used here is

$$\mathbb{F}\{U_i(x, y, z)\} = \bar{U}_i(k_1, k_2, z), \qquad \mathbb{F}\{F_i(x, y, z)\} = \bar{F}_i(k_1, k_2, z), \tag{33}$$

and all operational properties can be deduced from those of the single Fourier transform.

Application of the aforementioned double Fourier transform to equation (28) written in expanded form yields the following system of equations:

$$\frac{\mathrm{d}^2}{\mathrm{d}z^2}\bar{U}_x - 2\mathrm{i}k_1\frac{\mathrm{d}}{\mathrm{d}z}\bar{U}_z + (-3k_1^2 - k_2^2 + \omega^2\alpha^2(z))\bar{U}_x - 2k_1k_2\bar{U}_y = -\alpha^2(z)\bar{F}_x,$$

$$\frac{\mathrm{d}^2}{\mathrm{d}z^2}\bar{U}_y - 2\mathrm{i}k_2\frac{\mathrm{d}}{\mathrm{d}z}\bar{U}_z - 2k_1k_2\bar{U}_x + (-k_1^2 - 3k_2^2 + \omega^2\alpha^2(z))\bar{U}_y = -\alpha^2(z)\bar{F}_y,$$

$$-2\mathrm{i}k_1\frac{\mathrm{d}}{\mathrm{d}z}\bar{U}_x - 2\mathrm{i}k_2\frac{\mathrm{d}}{\mathrm{d}z}\bar{U}_y + 3\frac{\mathrm{d}^2}{\mathrm{d}z^2}\bar{U}_z + (-k_1^2 - k_2^2 + \omega^2\alpha^2(z))\bar{U}_z = -\alpha^2(z)\bar{F}_z, \tag{34}$$

where indicial notation has been abandoned and $\mathbf{x} = (x_1, x_2, x_3)$ is replaced by (x, y, z).

In order to reformulate equation (34) as a system consisting of three first order, ordinary differential equations [35], we introduce the notation

$$\bar{W}_x = \frac{\mathrm{d}}{\mathrm{d}z}\bar{U}_x, \qquad \bar{W}_y = \frac{\mathrm{d}}{\mathrm{d}z}\bar{U}_y \qquad \text{and} \qquad \bar{W}_z = \frac{\mathrm{d}}{\mathrm{d}z}\bar{U}_z. \tag{35}$$

Then, equation (34) becomes

$$\begin{aligned}
&\frac{\mathrm{d}}{\mathrm{d}z}\bar{W}_x - 2\mathrm{i}k_1\,\bar{W}_z + q_1^2(z)\bar{U}_x - 2k_1 k_2\,\bar{U}_y = -\alpha^2(z)\bar{F}_x,\\
&\frac{\mathrm{d}}{\mathrm{d}z}\bar{W}_y - 2\mathrm{i}k_2\,\bar{W}_z - 2k_1 k_2\,\bar{U}_x + q_2^2(z)\bar{U}_y = -\alpha^2(z)\bar{F}_y,\\
&-2\mathrm{i}k_1\,\bar{W}_x - 2\mathrm{i}k_2\,\bar{W}_y + 3\frac{\mathrm{d}}{\mathrm{d}z}\bar{W}_z + q_3^2(z)\bar{U}_z = -\alpha^2(z)\bar{F}_z,
\end{aligned} \tag{36}$$

where q_1 through q_3 are position-dependent, transformed wavenumbers (in m^{-1}), defined as

$$\begin{aligned}
q_1^2(z) &= -3k_1^2 - k_2^2 + \omega^2\alpha^2(z), \qquad q_2^2(z) = -k_1^2 - 3k_2^2 + \omega^2\alpha^2(z),\\
q_3^2(z) &= -k_1^2 - k_2^2 + \omega^2\alpha^2(z).
\end{aligned} \tag{37}$$

The next step is to combine equations (35) and (36) and introduce matrix notation. Thus, we obtain the following 6×6 first order differential equation system:

$$\frac{\mathrm{d}}{\mathrm{d}z}\begin{Bmatrix}\bar{U}_x\\ \bar{U}_y\\ \bar{U}_z\\ \bar{W}_x\\ \bar{W}_y\\ \bar{W}_z\end{Bmatrix} = \begin{bmatrix} & & [\mathbf{0}] & & & [\mathbf{I}] \\ -q_1^2(z) & 2k_1 k_2 & 0 & 0 & 0 & 2\mathrm{i}k_1\\ 2k_1 k_2 & -q_2^2(z) & 0 & 0 & 0 & 2\mathrm{i}k_2\\ 0 & 0 & -q_3^2(z)/3 & \tfrac{2}{3}\mathrm{i}k_1 & \tfrac{2}{3}\mathrm{i}k_2 & 0 \end{bmatrix} \begin{Bmatrix}\bar{U}_x\\ \bar{U}_y\\ \bar{U}_z\\ \bar{W}_x\\ \bar{W}_y\\ \bar{W}_z\end{Bmatrix} - \alpha^2(z)\begin{Bmatrix}0\\0\\0\\ \bar{F}_x\\ \bar{F}_y\\ \bar{F}_z/3\end{Bmatrix}, \tag{38}$$

where [**0**] and [**I**] are the null and unit submatrices, respectively. Using symbolic notation, equation (38) can be written as

$$\frac{\mathrm{d}}{\mathrm{d}z}\{\bar{\mathbf{V}}\} = [\mathbf{A}(z)]\{\bar{\mathbf{V}}\} + \{\bar{\mathbf{X}}\} \tag{39}$$

in the (k_1, k_2) Fourier domain. Since system matrix [**A**] is non-constant, the usual solution methodology for first order differential equation systems involving the eigenproperties of [**A**] is not applicable and special techniques (series expansions, Picard iterations) must be sought [35]. Solution of equation (39) for vector $\bar{\mathbf{V}}(k_1, k_2, z)$ must, of course, be followed by a double inverse Fourier transformation so as to return to the original spatial domain, i.e., to $\mathbf{V}(x, y, z)$.

The presence of the generalized (point) load vector $\{\bar{\mathbf{X}}\}$ greatly complicates the solutions procedure, so that it becomes necessary to convert it to equivalent initial conditions defined at $z = 0$. In particular,

$$\begin{Bmatrix} F_x \\ F_y \\ F_z \end{Bmatrix} = F_0\,\delta(x)\begin{Bmatrix} 1 \\ 1 \\ 1 \end{Bmatrix} = F_0\,\delta(x)\delta(y)\delta(z)\mathbf{e}, \tag{40}$$

so that the double Fourier transform yields

$$\begin{Bmatrix} \bar{F}_x \\ \bar{F}_y \\ \bar{F}_y \end{Bmatrix} = F_0\,\delta(z)\mathbf{e}. \tag{41}$$

From the theory of generalized functions [36], we know that solution $\mathscr{E}(z)$ of the nth order ordinary differential equation

$$\mathrm{D}^n\{\mathscr{E}(z)\} = \mathscr{E}^{(n)} + \alpha_1(z)\mathscr{E}^{(n-1)} + \alpha_2(z)\mathscr{E}^{(n-2)} + \cdots + \alpha_n(z)\mathscr{E} = \delta(z) \tag{42}$$

with zero initial conditions can be written as

$$\mathscr{E}(z) = H(z)\tilde{\mathscr{E}}(z), \tag{43}$$

where $H(z)$ is the Heaviside function and $\tilde{\mathscr{E}}(z)$ is the solution to the homogeneous version of equation (42) subject to the following initial conditions:

$$\tilde{\mathscr{E}}^{(n-1)}(0) = 1, \qquad \tilde{\mathscr{E}}^{(n-2)}(0) = \cdots = \tilde{\mathscr{E}}^{(1)}(0) = \tilde{\mathscr{E}}(0) = 0. \tag{44}$$

Thus, equation (39) can be recast as

$$\frac{\mathrm{d}}{\mathrm{d}z}\{\bar{\mathbf{V}}\} = [\mathbf{A}(z)]\{\bar{\mathbf{V}}\}, \qquad \{\bar{\mathbf{V}}(z=0)\} = \{\mathring{\mathbf{V}}\}, \tag{45}$$

where the equivalent initial condition vector is defined as

$$\{\mathring{\mathbf{V}}\}^{\mathrm{T}} = -F_0\,\alpha_0^2\,[0, 0, 0, 1, 1, 1/3], \tag{46}$$

with wave slowness $\alpha_0 = \alpha\,(z = 0)$. The solution procedure for equation (45) is elaborated in the next section.

5. FIRST ORDER MATRIX DIFFERENTIAL EQUATION SOLUTION

A closed form solution for a general first order $m \times m$ matrix differential equation system with both forcing function $\{\bar{\mathbf{X}}\}$ and initial conditions $\{\mathring{\mathbf{V}}\}$ is well known for system matrix $[\mathbf{A}]$ being constant [35]; i.e.,

$$\{\bar{\mathbf{V}}\} = \exp([\mathbf{A}]z)\left\{\{\mathring{\mathbf{V}}\} + \int_0^z \exp(-[\mathbf{A}]\zeta)\{\bar{\mathbf{X}}\}\,\mathrm{d}\zeta\right\}, \tag{47}$$

where exp is the exponential matrix function. A more elegant solution which avoids an expansion of the matrix exponential is through an eigenvalue analysis; i.e.,

$$[\mathbf{A}]\{\boldsymbol{\varphi}\}_i = \lambda_i\,\{\boldsymbol{\varphi}\}_i \qquad (i = 1, 2, \ldots, m) \tag{48}$$

(no summation implied), where λ_i are eigenvalues and $\{\boldsymbol{\varphi}\}_i$ are their corresponding eigenvectors. The use of these eigenproperties allows for diagonalization of [**A**] and easy computation of the matrix exponential, so that

$$\{\bar{\mathbf{V}}\} = \left(\sum_{i=1}^{m} \exp(\lambda_i z) \{\boldsymbol{\varphi}\}_i \{\boldsymbol{\psi}\}_i^{\mathrm{T}} \right) \{\mathring{\mathbf{V}}\} \tag{49}$$

in the absence of a forcing function. In the above, $\{\boldsymbol{\psi}\}_i$ are eigenvectors of $[\mathbf{A}]^{\mathrm{T}}$, with superscript T denoting transposition, an operation which leaves the eigenvalues unchanged. The above solution methodology can be used for the homogeneous medium case or within the context of transfer matrices for wave propagation through horizontally stratified, layered media. The general case of the heterogeneous medium where dependence of the wavenumbers on depth results in a non-constant system matrix [**A**] requires different techniques such as series expansions or Picard iterations [35]. Previous work [32] has shown the former technique to be somewhat more effective than the latter and will therefore be used herein. In this approach, both system matrix and response in the homogeneous version given by equation (45) (since the forcing function is expressed in terms of non-zero initial conditions) are expanded as polynomials in z; i.e.,

$$\{\bar{\mathbf{V}}(z)\} = \{\bar{\mathbf{V}}\}_0 + \{\bar{\mathbf{V}}\}_1 z + \{\bar{\mathbf{V}}\}_2 z^2 + \cdots \qquad \text{and} \qquad [\mathbf{A}(z)] = [\mathbf{A}]_0 + [\mathbf{A}]_1 z + [\mathbf{A}]_2 z^2 + \cdots, \tag{50}$$

where subscripts denote the expansion order. By substituting the above in equation (45) and matching powers of z, we obtain the following system:

$$[\mathbf{A}]_0\{\bar{\mathbf{V}}\}_0 = \{\bar{\mathbf{V}}\}_1, \qquad [\mathbf{A}]_0 \{\bar{\mathbf{V}}\}_1 + [\mathbf{A}]_1 \{\bar{\mathbf{V}}\}_0 = 2\{\bar{\mathbf{V}}\}_2,$$
$$[\mathbf{A}]_0 \{\bar{\mathbf{V}}\}_2 + [\mathbf{A}]_1 \{\bar{\mathbf{V}}\}_1 + [\mathbf{A}]_2 \{\bar{\mathbf{V}}\}_0 = 3\{\bar{\mathbf{V}}\}_3, \tag{51}$$

etc. By identifying the zeroth order solution with initial conditions $\{\mathring{\mathbf{V}}\}$, the first and higher order solutions are obtained, as

$$\{\bar{\mathbf{V}}\}_1 = [\mathbf{A}]_0 \{\mathring{\mathbf{V}}\}, \qquad \{\bar{\mathbf{V}}\}_2 = \tfrac{1}{2}([\mathbf{A}]_1 + [\mathbf{A}]_0^2)\{\mathring{\mathbf{V}}\} = [\mathbf{B}]_0 \{\mathring{\mathbf{V}}\},$$
$$\{\bar{\mathbf{V}}\}_3 = \tfrac{1}{3}([\mathbf{A}]_2 + [\mathbf{A}]_1 [\mathbf{A}]_0 + \tfrac{1}{2}[\mathbf{A}]_0 [\mathbf{A}]_1 + \tfrac{1}{2}[\mathbf{A}]_0^3)\{\mathring{\mathbf{V}}\} = \tfrac{1}{3}([\mathbf{A}]_2 + [\mathbf{A}]_1 [\mathbf{A}]_0 + [\mathbf{A}]_0 [\mathbf{B}]_0) = [\mathbf{C}]_0 \{\mathring{\mathbf{V}}\}. \tag{52}$$

The final response can then be reconstituted through recourse to equation (50) as

$$\{\bar{\mathbf{V}}\} = ([\mathbf{I}] + [\mathbf{A}]_0 z + [\mathbf{B}]_0 z^2 + [\mathbf{C}]_0 z^3 + \cdots)\{\mathring{\mathbf{V}}\}, \tag{53}$$

where [**I**] is the identity matrix. This type of approach favors a polynomial (in z) structure of the transformed wavenumbers q_1–q_3 which, in turn, depend on the wavespeed slowness $\alpha(z)$. Recourse to equations (21), (25) and (37) indicates three typical structures, depending on constant, linear or quadratic density profiles. Thus, wavespeed slowness has the general form

$$\alpha(z) = \alpha_0 (az + 1)^{-n/2}, \tag{54}$$

where $n = 0, 1, 2$, respectively, correspond to the quadratic, linear and constant density profiles, while constant $a = (\sqrt{\mu_1}/\sqrt{\mu_0} - 1)/L$ (in m^{-1}) is discussed within the context of heterogeneous media representations in the next section. The consequence of the above equation is that the transformed wavenumbers assume the form

$$q_i^2 = -Q_i^2 + k_0^2 \alpha^2(z)/\alpha_0^2 = -Q_i^2 + k_0^2 (az + 1)^{-n}, \qquad i = 1, 2, 3, \tag{55}$$

where $k_0^2 = \omega^2\alpha_0^2$, $Q_1^2 = 3k_1^2 + k_2^2$, $Q_2^2 = k_1^2 + 3k_2^2$, $Q_3^2 = k_1^2 + k_2^2$ and $\alpha(z)$ is the appropriate wave slowness profile.

If $n = 0$ we have a macroscopically homogeneous medium and all three transformed wavenumbers are constants. In this case, the expansion of $[\mathbf{A}(z)]$ has one term, namely

$$[\mathbf{A}]_0 = \begin{bmatrix} & [\mathbf{0}] & & [\mathbf{I}] \\ Q_1^2 - k_0^2 & 2k_1 k_2 & 0 & \\ 2k_1 k_2 & Q_2^2 - k_0^2 & 0 & [\mathbf{D}] \\ 0 & 0 & \frac{1}{3}(Q_3^2 - k_0^2) & \end{bmatrix}, \tag{56}$$

where

$$[\mathbf{D}] = \begin{bmatrix} 0 & 0 & 2ik_1 \\ 0 & 0 & 2ik_2 \\ \frac{2}{3}ik_1 & \frac{2}{3}ik_2 & 0 \end{bmatrix}, \tag{57}$$

while

$$[\mathbf{A}]_1 = [\mathbf{A}]_2 = [\mathbf{0}]. \tag{58}$$

If $n = 1$, we have a heterogeneous medium with a wavespeed varying as the square root of a linear function in the depth co-ordinate. An expansion of the corresponding wavenumbers in terms of z (keeping in mind that $az < 1{\cdot}0$, as discussed in the next section) yields the following terms (where $[\mathbf{A}]_0$ is the same as before):

$$[\mathbf{A}]_1 = \begin{bmatrix} & [\mathbf{0}] & & [\mathbf{0}] \\ ak_0^2 & 0 & 0 & \\ 0 & ak_0^2 & 0 & [\mathbf{0}] \\ 0 & 0 & \frac{1}{3}ak_0^2 & \end{bmatrix} \tag{59}$$

and

$$[\mathbf{A}]_2 = \begin{bmatrix} & [\mathbf{0}] & & [\mathbf{0}] \\ -(ak_0)^2 & 0 & 0 & \\ 0 & -(ak_0)^2 & 0 & [\mathbf{0}] \\ 0 & 0 & -\frac{1}{3}(ak_0)^2 & \end{bmatrix}. \tag{60}$$

Finally, if $n = 2$ we have a heterogeneous medium with a linearly varying wavespeed, and the expansions terms ($[\mathbf{A}]_0$ same as before) are

$$[\mathbf{A}]_1 = \begin{bmatrix} & [\mathbf{0}] & & [\mathbf{0}] \\ 2ak_0^2 & 0 & 0 & \\ 0 & 2ak_0^2 & 0 & [\mathbf{0}] \\ 0 & 0 & \frac{2}{3}ak_0^2 & \end{bmatrix} \tag{61}$$

and

$$[\mathbf{A}]_2 = \begin{bmatrix} & [\mathbf{0}] & & [\mathbf{0}] \\ -3(ak_0)^2 & 0 & 0 & \\ 0 & -3(ak_0)^2 & 0 & [\mathbf{0}] \\ 0 & 0 & -(ak_0)^2 & \end{bmatrix}. \tag{62}$$

With the expansion terms of $[\mathbf{A}(z)]$ now available, equation (52) can be used to synthesize matrices $[\mathbf{B}]_0$ and $[\mathbf{C}]_0$, while equation (53) gives the solution for $\{\overline{\mathbf{V}}\}$ in terms of the initial conditions $\{\mathring{\mathbf{V}}\}$. Also, since this is essentially a series expansion technique, there is an inevitable loss of accuracy for large values of z. The method, however, is general enough to handle polynomial type variation in the wavenumbers $q_1(z)$–$q_3(z)$. Finally, solution of the simpler scalar wave equations using a first order, matrix differential equation system was completed by the authors in a previous publication [32].

5.1. INVERSE FOURIER TRANSFORMATIONS

The previously developed solution methodology is defined in a doubly transformed Fourier domain (k_1, k_2), where k_1 and k_2 are wavenumbers (in m^{-1}). Thus, the final step in this solution procedure is a numerical inverse transformation of solution vector $\{\overline{\mathbf{V}}\}$ given by equation (53) back to the spatial (x, y) domain, so as to recover the displacement components U_x, U_y and U_z corresponding to a forcing function which is a point impulse in space and time harmonic. One last scaling is required, as dictated by the algebraic transformation procedure and given by equation (9). Thus, we obtain a solution vector $\mathbf{u}(\mathbf{x}, \omega) = [u_x, u_y, u_z]^{\mathrm{T}}$ for each of the three point impulses, which is actually a Green function $g_{ij}(\mathbf{x}, \omega)$, $i, j = 1, 2, 3$, for the time harmonic vector wave equation defined in a heterogeneous medium with a Poisson ratio of 0·25, a quadratic shear modulus profile in depth and a choice of constant, linear or quadratic density profiles.

The direct/inverse multiple Fourier transformation software package given in reference [37] was employed herein for the inversion part. It was extensively tested regarding correct implementation of its storage structure for both direct and inverse, single and double Fourier transformations. One of the example functions used is

$$f(x, y) = \frac{\sin kx}{x} \frac{\sin ky}{y}, \tag{63}$$

the double Fourier transform of which is

$$\overline{f}(k_1, k_2) = \begin{cases} \pi^2 & \text{if } |k_1|, |k_2| \leqslant k \text{ (real)}, \\ 0 & \text{otherwise.} \end{cases} \tag{64}$$

The FFT inversion of equation (64) employed a square mesh of size $N^2 = 64^2 = 4096$, which was chosen as representing a compromise between an $N^2 = 32^2 = 1024$ point mesh, which is too crude, and an $N^2 = 128^2 = 16\,384$ point mesh, which becomes cumbersome to use.

In order to reproduce the same conditions as those for the numerical examples in section 7, the horizontal square grid (x, y) had dimension l ranging from λ_s to $8\lambda_s$, λ_s being the shear wavelength for limestone material at $\omega = 10$ Hz; i.e., $\lambda_s = 308{\cdot}6$ m. Constant k was identified with the shear wavenumber at the same frequency; i.e., $k = k_s = 0{\cdot}0204\ \mathrm{m}^{-1}$. Results obtained for four mesh dimensions, both in terms of sampled functions $\overline{f}(k_1, k_2)$ and inverted function $f(x, y)$ at $k_2 = 0$ for the former and at $y = 0$ for the latter, are plotted in Figure 2. As far as sampling in the transformed wavenumber domain is concerned, we observe that an increase in the dimensions of the corresponding spatial mesh $(|x| \leqslant l/2, |y| \leqslant l/2)$ results in a decrease in the size of the transformed mesh $(|k_1| \leqslant K, |k_2| \leqslant K)$ which, for fixed k, yields a better representation of $\overline{f}(k_1, k_2)$. In Table 1 is shown the relation between the dimensions of both (x, y) and (k_1, k_2) meshes for the cases examined in Figure 2, where $\Delta x = \Delta y = l/N$, $\Delta k_1 = \Delta k_2 = 2K/N$ and $K = 2\pi/(2\Delta x) = \pi/\Delta y$.

In all cases, the variation of the recovered function f with respect to co-ordinates x and y is well reproduced for $N^2 = 4096$ data points. It is the magnitude of f, however, which is dependent on the size of the sampling mesh. We note that, at the center of the mesh,

$$\lim_{x,y\to 0} f(x, y) = (k \cos x)\,(k \cos y) = k^2 \tag{65}$$

represents the maximum value for f. In Table 2 it is depicted how this maximum value improves rapidly with increasing mesh size until the $l = 6\lambda_s$ mesh is reached, past which further improvement is rather minor. Therefore, for $N^2 = 4096$ sampling points, the square mesh of dimension $l = 6\lambda_s$ appears as optimal and yields a solution which is in error by 4·2% for k. Any further improvement would require moving to $N^2 = 16\,384$ sampling points.

6. WAVESPEED PROFILES FOR THE HETEROGENEOUS MEDIUM

The various constraints that appeared during the solution procedure for the equations of elastodynamics will now be examined in detail. At first, it was established in section 3 that the elastic parameter profiles are quadratic functions of depth co-ordinate $z = x_3$, as given by equation (21), and that $\nu = 0{\cdot}25$. The constants c_0 and c_1 can be determined from values at two reference locations, namely $z = 0$ and $z = L$, which in a Green function solution can be identified with the depth co-ordinates of the source and the receiver. Therefore, given that $\mu(0) = \mu_0$ and $\mu(L) = \mu_1$, we have that

$$\lambda(z) = \mu(z) = \{(\sqrt{\mu_1} - \sqrt{\mu_0})\,(z/L) + \sqrt{\mu_0}\}^2. \tag{66}$$

Next, the density profile must be established. We will consider the following three cases:

$$\varrho(z) = \varrho_0, \qquad \varrho(z) = \varrho_0 \left\{\left(\frac{\sqrt{\varrho_1}}{\sqrt{\varrho_0}} - 1\right)(z/L) + 1\right\},$$

$$\varrho(z) = \varrho_0 \left\{\left(\frac{\sqrt{\varrho_1}}{\sqrt{\varrho_0}} - 1\right)(z/L) + 1\right\}^2, \tag{67}$$

corresponding to constant, linear and quadratic depth profiles. As before, subscripts 0 and 1 respectively correspond to the surface and to layer depth L. Assuming, for convenience, that the rate of increase of the shear modulus is proportional to that of the density (i.e., $\mu_1/\mu_0 = \varrho_1/\varrho_0$ for the quadratic case and $\sqrt{\mu_1}/\sqrt{\mu_0} = \varrho_1/\varrho_0$ for the linear case), then the corresponding shear wave profiles are

$$c_s(z) = c_{s0} \left\{\left(\frac{\sqrt{\mu_1}}{\sqrt{\mu_0}} - 1\right)(z/L) + 1\right\},$$

$$c_s(z) = c_{s0} \sqrt{\left(\frac{\sqrt{\mu_1}}{\sqrt{\mu_0}} - 1\right)(z/L) + 1},$$

$$c_s(z) = c_{s0} = \sqrt{\mu_0/\varrho_0}, \tag{68}$$

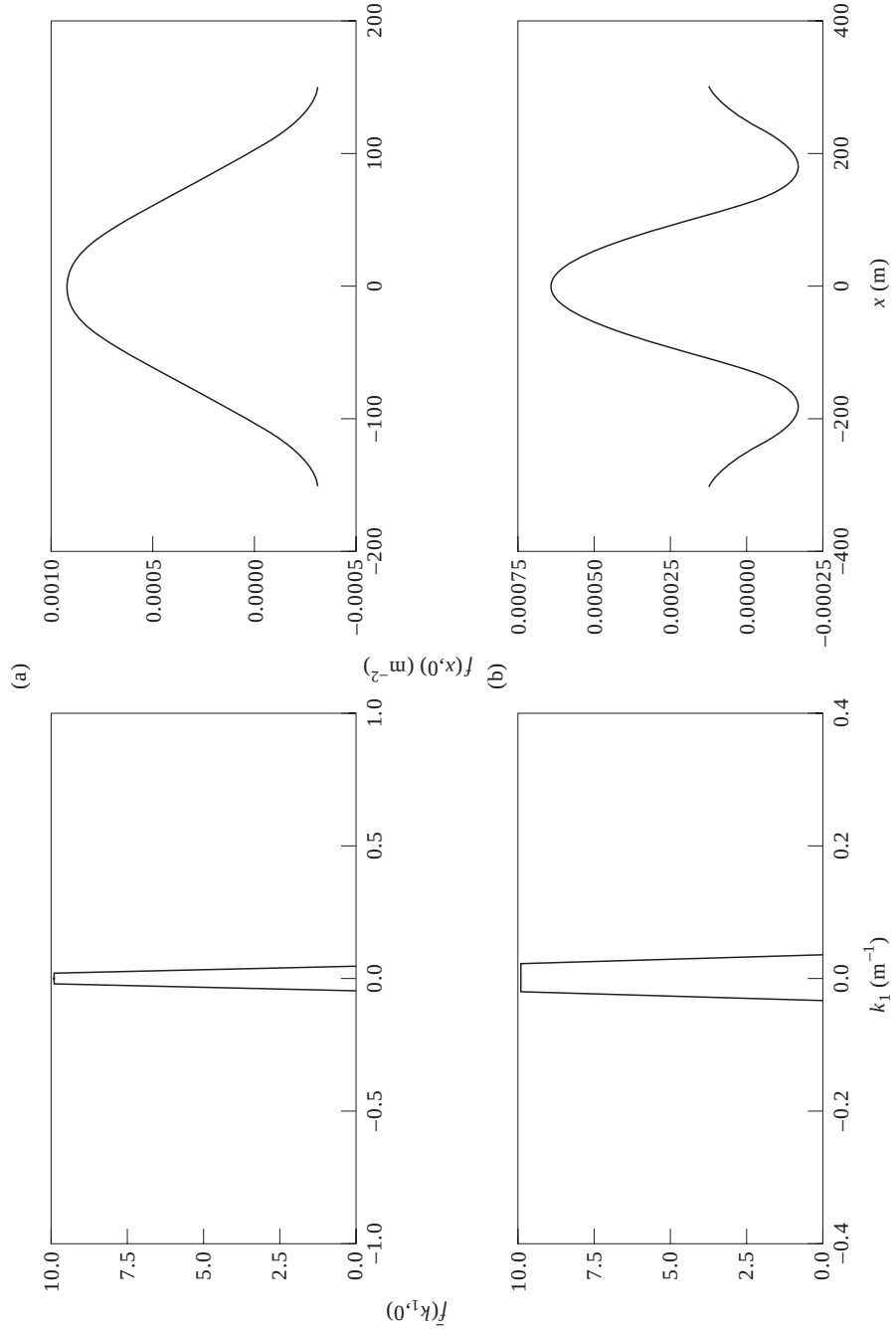

Figure 2. (a) and (b)

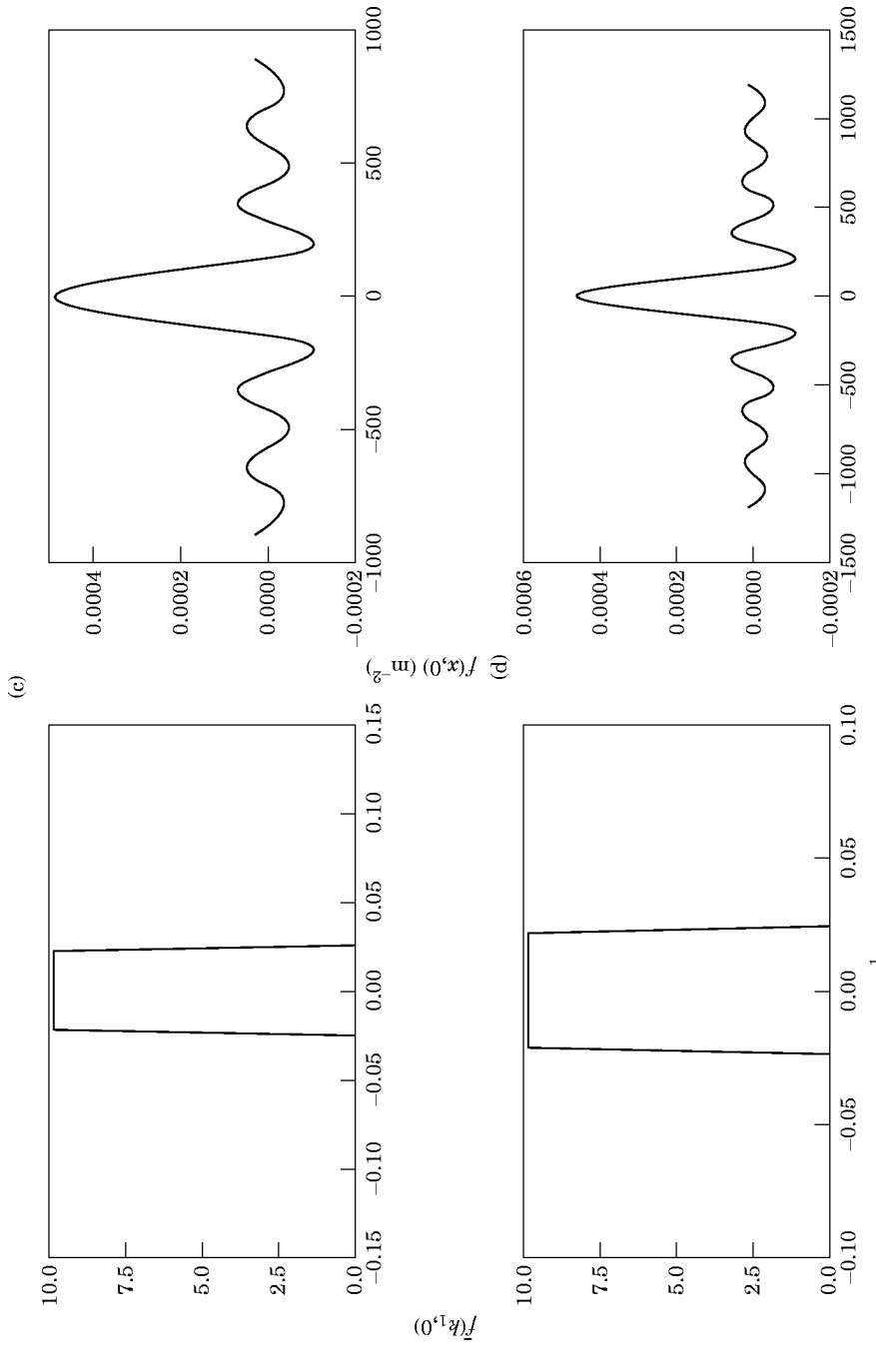

Figure 2. The original and inverted trial functions f for a square mesh of size l equal to (a) λ_s, (b) $2\lambda_s$, (c) $6\lambda_s$ and (d) $8\lambda_s$.

TABLE 1

Details of mesh dimensions in spatial and transformed wavenumber domains for $N^2 = 4096$ points

l (m)	$\Delta x = \Delta y$ (m)	$\Delta k_1 = \Delta k_2$ (m^{-1})	K (m^{-1})
308·6	4·822	$0{\cdot}2035 \times 10^{-1}$	0·6515
617·2	9·644	$0{\cdot}1017 \times 10^{-1}$	0·3257
1852	28·93	$0{\cdot}3393 \times 10^{-2}$	0·1085
2469	38·58	$0{\cdot}2544 \times 10^{-2}$	$0{\cdot}8143 \times 10^{-1}$

while $c_p(z) = \sqrt{3}c_s(z)$. The first case is depicted in Figure 3. Finally, the wave slowness $\alpha(z)$ is the inverse of the shear wave speed and can be written in the following general form:

$$\alpha^2(z) = (\varrho_0/\mu_0)\left\{\left(\frac{\sqrt{\mu_1}}{\sqrt{\mu_0}} - 1\right)(z/L) + 1\right\}^{-n}$$

$$= \alpha_0^2\{az + b\}^{-n}, \tag{69}$$

where $a = (\sqrt{\mu_1}/\sqrt{\mu_0} - 1)/L$ and $b = 1$. The case $n = 0$ corresponds to a constant wave slowness that results from combining the quadratic shear modulus and density profiles and results in a macroscopically homogeneous medium. Cases $n = 1$ and $n = 2$ correspond to wave slowness that vary inversely as the square root and as a linear function of depth, respectively, and are due to linear and to constant density profiles in combination with the quadratic shear modulus.

6.1. VISCOELASTIC MATERIAL BEHAVIOUR

In order to simulate energy absorption and dispersion phenomena which are associated with wave propagation, it is necessary to introduce elements from the theory of viscoelasticity [38]. Specifically, if the simple three-parameter solid is introduced within the context of time harmonic conditions, then the elastic shear modulus μ in the present formulation is replaced by a complex impedance function $\mu_v(\omega)$, with real and imaginary parts given by

$$\text{Re}\{\mu_v(\omega)\} = (q_0^2 + \omega^2 q_1^2)/(1 + \omega^2 p_1^2),$$

$$\text{Im}\{\mu_v(\omega)\} = (\omega(q_1 - q_0 p_1)/(1 + \omega^2 p_1^2). \tag{70}$$

In the above q_0, q_1 and p_1 are material constants (not to be confused with the transformed wavenumbers $q_i(z)$) for which the inequality $q_1 > p_1 q_0$ must hold for physical reasons. Special cases include the Maxwell fluid ($q_0 = 0$) and the Kelvin solid ($p_1 = 0$). In order to remain consistent with the previous development, μ_0 and μ_1 in equation (66) are identified with values of $\mu_v(\omega)$ at $z = 0$ and $z = L$, respectively, while the density profile in equation (67) remains real and depends on values of μ_0 and μ_1 for the linear elastic case. A direct consequence of the use of viscoelastic moduli is that the wavespeeds have complex, frequency dependent structure which filters into their wavenumbers. Thus, amplitude reduction associated with absorption can be captured due to the presence of imaginary components in the wavenumbers, while dispersion effects are automatically included in any frequency-dependent representation of the wavespeeds.

7. NUMERICAL EXAMPLES

In this section, wave propagation due to a point source in a continuously heterogeneous geological medium is examined by using the present methodology. In particular, we consider naturally occurring limestone with the following range of material properties [2]:

$$\varrho = 2100\text{–}2800\ \text{kg/m}^3, \qquad \mu = (0{\cdot}2\text{–}0{\cdot}3) \times 10^{11}\ \text{Pa}, \qquad \nu = 0{\cdot}25\text{–}0{\cdot}30. \tag{71}$$

Reference values at $z = 0$ (the source location) are

$$\mu_0 = 0{\cdot}2 \times 10^{11}\ \text{Pa}, \qquad \varrho_0 = 2100\ \text{kg/m}^3, \tag{72}$$

while at $z = 1$ (the bottom of the deposit) we have

$$\mu_1 = 0{\cdot}2667 \times 10^{11}\ \text{Pa}, \qquad \varrho_1 = 2800\ \text{kg/m}^3. \tag{73}$$

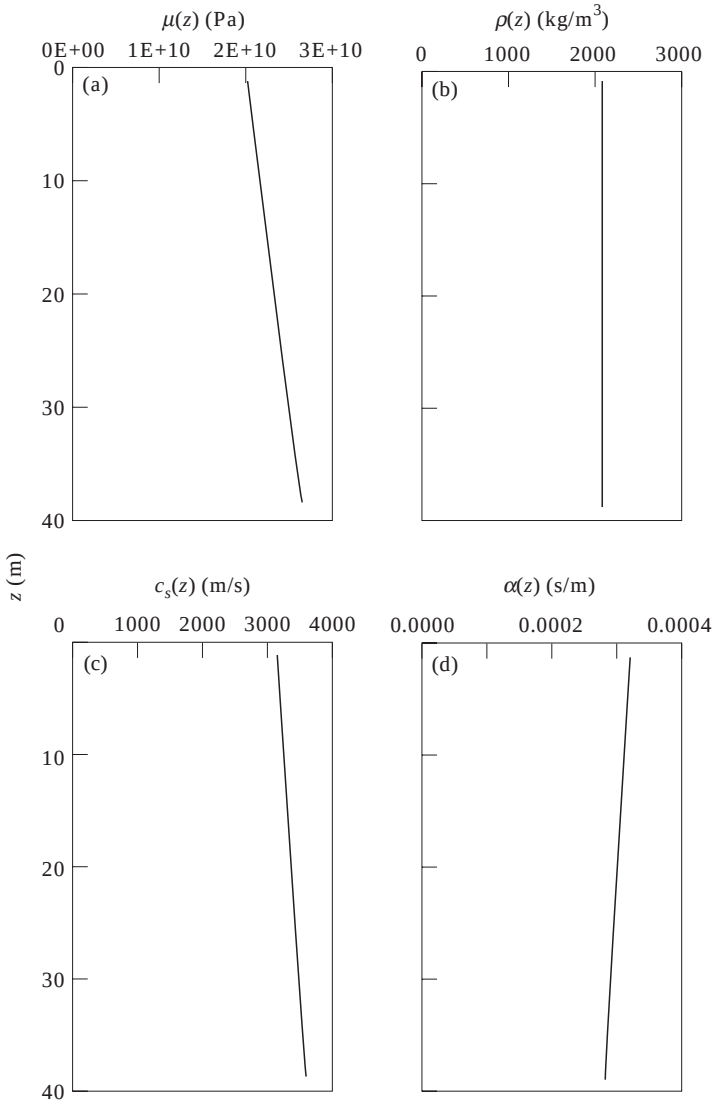

Figure 3. Material parameter depth profiles for $0 \leqslant z \leqslant 1$. (a) Shear modulus $\mu(z)$; (b) density $\varrho(z)$; (c) shear wavespeed $c_s(z)$; (d) the shear wave slowness $\alpha(z)$.

TABLE 2

Magnitude of $f(x, y)$ at center of mesh versus square mesh size l for $N^2 = 4096$ points

l (m)	$f(0, 0)$
308·6	$0{\cdot}9326 \times 10^{-3}$
617·2	$0{\cdot}6476 \times 10^{-3}$
1852	$0{\cdot}4864 \times 10^{-3}$
2469	$0{\cdot}4679 \times 10^{-3}$
Exact value	$0{\cdot}4145 \times 10^{-3}$

As discussed in section 3, the methodology requires that $\nu = 0{\cdot}25$, which results in $\lambda(z) = \mu(z)$. Furthermore,

$$c_{s0} = \sqrt{\mu_0 / \varrho_0} = 3086 \text{ ms} \qquad \text{and} \qquad c_{p0} = \sqrt{3} c_{s0} = 5345 \text{ m/s} \tag{74}$$

are reference values for the shear and pressure wavespeeds, respectively. We note at this point that for wave propagation under time harmonic conditions,

$$\lambda = 2\pi/k = 2\pi c/\omega \tag{75}$$

where wavelength λ, wavenumber k and wavespeed c are identified with either P or S waves. Since the frequency range in which most of seismically induced wave energy is concentrated is in the 0·2–25 Hz band, we will consider an intermediate frequency $f = 10$ Hz. In Table 3 are listed values for wavelengths λ and wavenumbers k corresponding to the above reference values. Of the three possible density profiles given by equation (67), we will focus on the constant one ($\varrho_0 = \varrho_1 = 2100 \text{ kg/m}^3$) which results in a linear wavespeed profile with respect to depth z, as shown in Figure 3.

Prior to investigating a Green function for the special type of heterogeneous medium developed in sections 3–5, the Fourier transform grid was calibrated using the simpler case of uni-dimensional (scalar) wave propagation, for which the Green function corresponding to outgoing waves from a point source in the three-dimensional continuum is

$$g(x, y, z) = \frac{1}{4\pi r} \exp(k_0 r), \qquad r^2 = x^2 + y^2 + z^2, \tag{76}$$

with

$$\bar{g}(k_1, k_2, z) = \frac{\sin\left(\sqrt{k_0^2 - k_1^2 - k_2^2}\,|z|\right)}{\sqrt{k_0^2 - k_1^2 - k_2^2}} \tag{77}$$

as its double Fourier transform with respect to (x, y). The depth of the non-homogeneous limestone deposit is related to the reference wavelength corresponding to shear waves ($\lambda_s = 308{\cdot}6$ m), while the size of the horizontal grid is determined by taking into account the information given in section 5.1. Specifically, for $N^2 = 64^2 = 4096$, a square space grid of dimension $l = 6\lambda_s = 1852$ (m) with length increments $\Delta x = \Delta y = l/N = 28{\cdot}93$ m is considered adequate. The size of the corresponding transformed wavenumber grid is

TABLE 3

Elastic waves in limestone under time-harmonic conditions; reference case

f(Hz)	ω(r/s)	λ_p (m)	λ_s (m)	k_p (1/m)	k_s (1/m)
10	62·83	534·5	308·6	0·01176	0·02036

TABLE 4

The magnitude of the numerically inverted scalar fundamental solution $g(x, y, z)$ at mesh co-ordinate $x = 0$ versus the exact solution for an $N^2 = 4096$ point mesh

	g (inverted) at $y = 0$ (m^{-1})	g (exact) at $y = 0$ (m^{-1})	Error (%)	g (inverted) at $y = 0{\cdot}75\lambda_s$ (m^{-1})	g (exact) at $y = 0{\cdot}75\lambda_s$ (m^{-1})	Error (%)
$z = 1{\cdot}5\lambda_s$	$0{\cdot}3713 \times 10^{-3}$	$0{\cdot}3438 \times 10^{-3}$	7·9	$-0{\cdot}6541 \times 10^{-4}$	$-0{\cdot}1361 \times 10^{-3}$	51·9
$z = 2{\cdot}0\lambda_s$	$-0{\cdot}2424 \times 10^{-3}$	$-0{\cdot}2578 \times 10^{-3}$	5·9	$-0{\cdot}1183 \times 10^{-3}$	$-0{\cdot}1585 \times 10^{-3}$	25·3

therefore $K = \pi/\Delta x = 0{\cdot}1085$ (1/m) and the sampling interval is $\Delta k_1 = \Delta k_2 = 2K/N = 0{\cdot}003393$ (1/m). We note that sampled function $\bar{g}(k_1, k_2, z)$ as well as inverted function $g(x, y, z)$ span both negative and positive values, i.e., $-K < k_1,\ k_2 \leqslant K$ and $-l/2 < x,\ y \leqslant l/2$, respectively. The relevant results are summarized in Table 4, where it is observed that: (i) the accuracy of the numerically inverted fundamental solution $g(x, y, z)$ does not depend on the depth co-ordinate; (ii) the results are best around the center of the horizontal grid ($y = 0$, $|x| \leqslant 3\lambda_s$); and (iii) the accuracy deteriorates as the periphery of the mesh is approached (e.g., $y > 0{\cdot}75\lambda_s$, $|x| \leqslant 3\lambda_s$).

We now investigate the Green function for the 3-D vector wave equation for a source (unit point impulses in the three principal directions) placed at the top surface ($z = 0$) of the elastic deposit and for receivers spanning 40 equal distances along the z-axis up to a depth $z = l = 0{\cdot}125\lambda_s = 38{\cdot}58$ m (note that signal decay is rapid with respect to distance). For this particular orientation of the axes and of the heterogeneity, $g_{11} = g_{22}$ and $g_{12} = g_{13} = g_{23} = 0$. Figures 4 and 5 yield information on the behavior of components g_{11} and g_{33} along a horizontal plane at fixed depth of $z = l$. We first note that the real parts of the sampled components $\bar{g}_{11}\,(k_1, k_2 = 0)$ and $\bar{g}_{33}\,(k_1, k_2 = 0)$ have a local minimum at $k_1 = k_2 = 0$ and cross the transformed axis at $k_1 = k_2 = \pm 0{\cdot}0625$ (1/m), respectively, which would be considered as singular points in a contour integration along the complex wavenumber plane [22]. The imaginary parts of $\bar{g}_{11}$ and $\bar{g}_{33}$ is zero and, as a result, the imaginary part of the corresponding inverted functions g_{11} and g_{33} is negligible. Thus, the inverse Fourier transform procedure in combination with the first order, matrix differential equation solution of the vector wave equation yields the amplitude of the Green function only. In order to recover the phase angle, it is necessary to resort a complex representation of the wavenumbers k_p and k_s according to the correspondence principle of viscoelasticity so as to produce a sizeable imaginary part in the component matrices $[\mathbf{A}]_0$, $[\mathbf{A}]_1$ and $[\mathbf{A}_2]$ of equation (53). Next, we observe certain similarities in the amplitude of the Green function between the heterogeneous and equivalent homogeneous media in that there is a peak around the center of the mesh (directly below the source) which decays with distance.

Next, in Figures 6 and 7 respectively are plotted components g_{11} and g_{33} (amplitude plus phase angle) versus depth z along with the difference (as a percentage) in these amplitudes between cases corresponding to the heterogeneous deposit and the equivalent homogeneous deposit with $\mu(z) = \mu_0$ and $\varrho(z) = \varrho_0$, which is used as the reference solution. It is observed that this difference increases almost linearly as the source to receiver distance becomes larger and, for the present configuration, attains a maximum value of about 15%. This behavior is consistent with the fact that in a continuously heterogeneous medium we have scattering due to changing material properties and, as a result, the wave signal deviates from what would be observed in an equivalent homogeneous medium at a rate which increases with distance. We note at this point that the difference in amplitude is

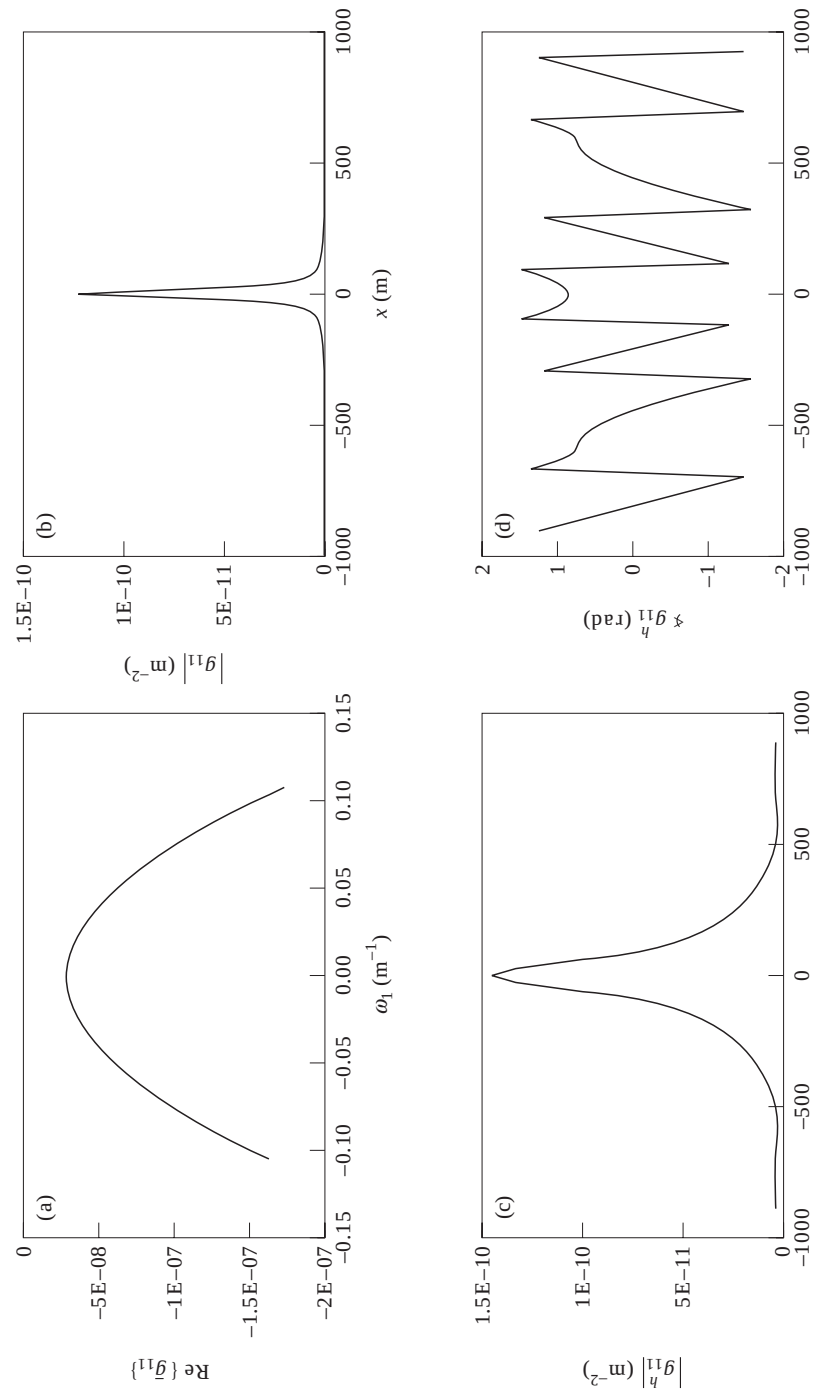

Figure 4. The fundamental solution component g_{11} at depth $z = 0{\cdot}125\lambda_s$. (a) The real part of the Fourier transform at $k_2 = 0$; (b) the amplitude of the inverted function at $y = 0$; (c) the amplitude and (d) the phase angle for the corresponding homogeneous medium.

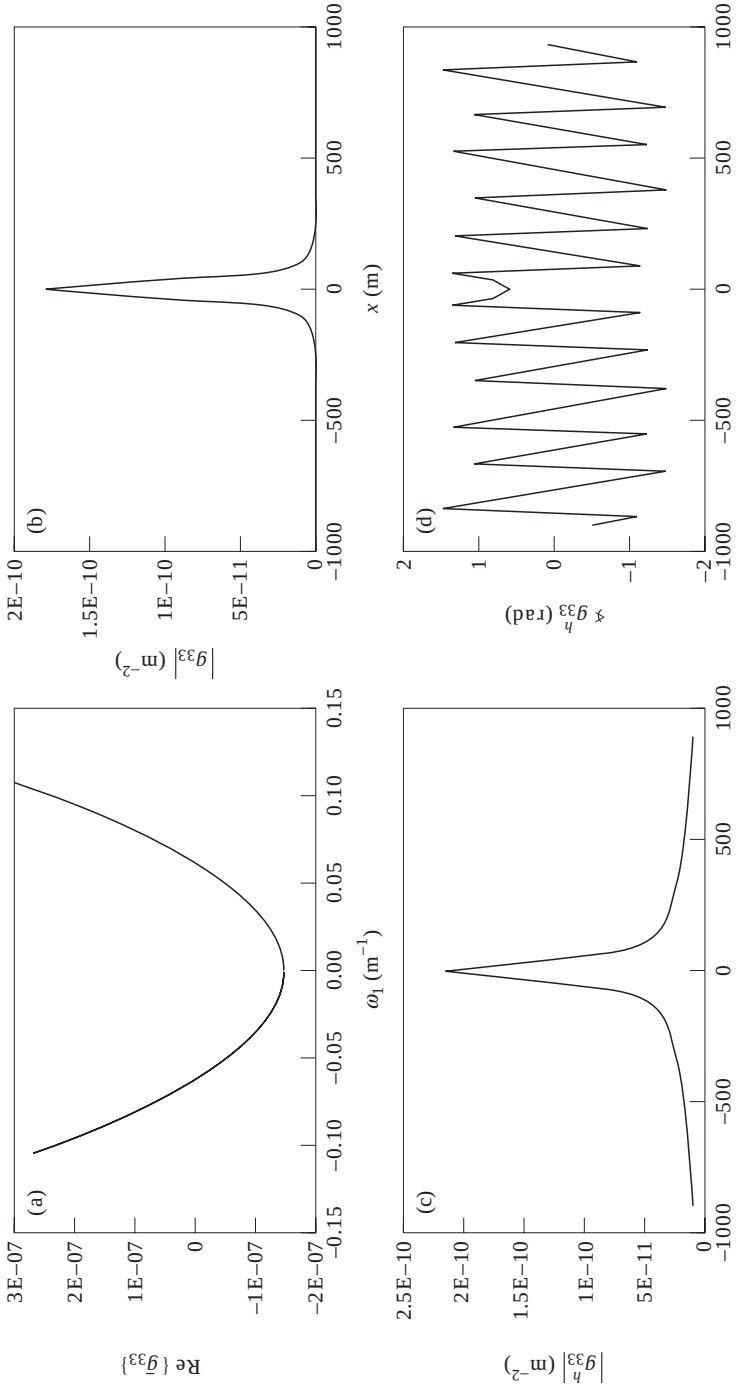

Figure 5. The fundamental solution component g_{33} at depth $z = 0{\cdot}125\lambda_s$. (a) The real part of the Fourier transform at $k_2 = 0$; (b) the amplitude of the inverted function at $y = 0$; (c) the amplitude and (d) the phase angle for the corresponding homogeneous medium.

roughly the same for both g_{11} (motions perpendicular to the z-axis) and g_{33} (motions parallel to the z-axis) components. Also, a negative amplitude difference indicates a displacement signal in the heterogeneous medium that is less pronounced compared to the one in the homogeneous medium. This de-amplification is a result of the deposit becoming stiffer in the direction of wave propagation.

Finally, the time-dependent responses for components g_{11} and g_{33} are shown in Figures 8 and 9, respectively. We employ the same fixed source–receiver configuration as that used in conjunction with Figures 4 and 5, except for the fact that the depth of the layer is now $l = c_{p0}/10 = 534$ m. Thus, the travel times for P and S waves to reach the source (using the reference wavespeeds of equation (74)) are $t_{p0} = 0{\cdot}10$ s and $t_{s0} = 0{\cdot}17$ s, respectively. The

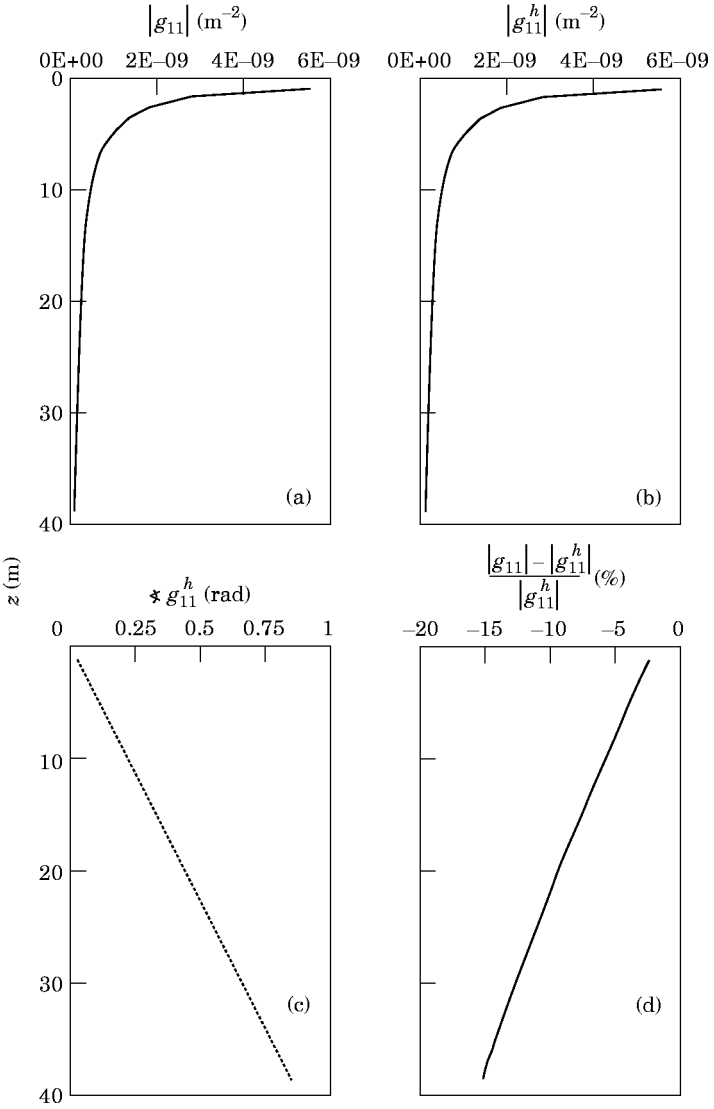

Figure 6. The fundamental solution component g_{11} versus depth z. (a) Amplitude, (b) amplitude and (c) phase angle for corresponding homogeneous medium and (d) percent difference in amplitude between heterogeneous and homogeneous media.

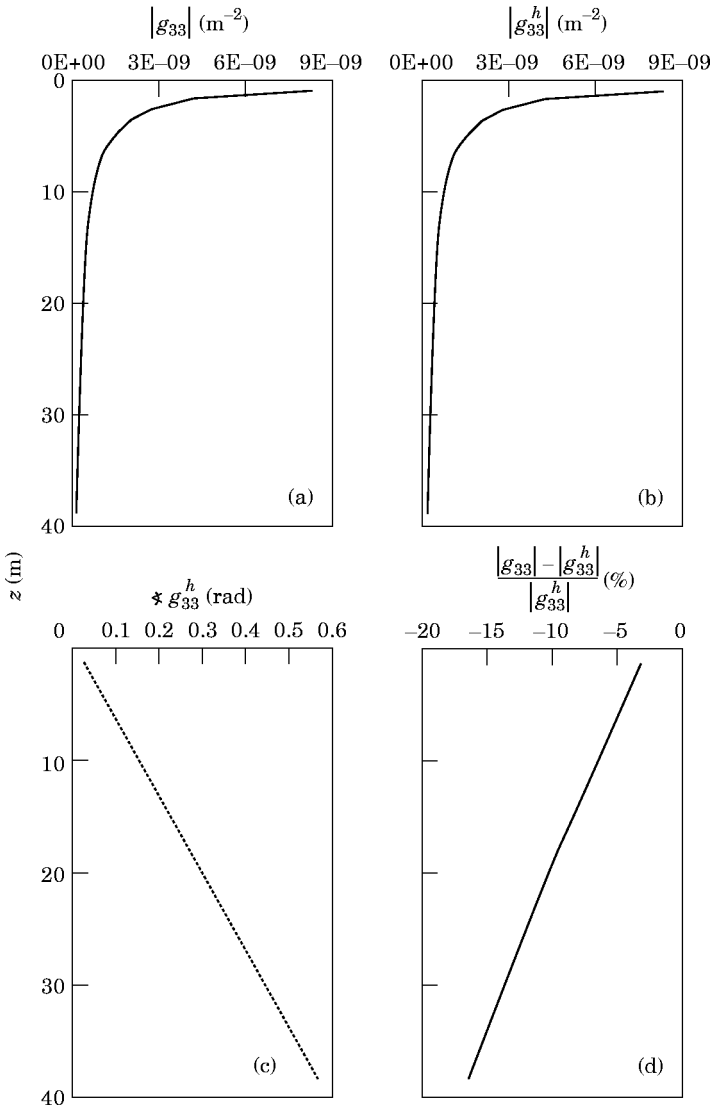

Figure 7. The fundamental solution component g_{33} vs depth z. (a) Amplitude, (b) amplitude and (c) phase angle for corresponding homogeneous medium and (d) percent difference in amplitude between heterogeneous and homogeneous media.

transient response is synthesized from a spectrum of values in the frequency ω domain at the receiver using the FFT [37] with

$$\Delta t = 0{\cdot}005 \text{ (s)}, \qquad T = 0{\cdot}64 \text{ (s)},$$
$$\Delta\omega = 4{\cdot}91 \text{ (rad/s)}, \qquad \Omega = 628{\cdot}5 \text{ (rad/s)}, \tag{78}$$

where $-\Omega < \Delta\omega \leqslant \Omega$ is the sampling interval and $-T < \Delta t \leqslant T$ is the time step, with $N = 256$ as the total number of samples. Furthermore, the discrete frequency and time domains are related as [37]

$$\Delta\omega = 2\pi/(N\Delta t) \qquad \text{and} \qquad \Omega = \pi/\Delta t. \tag{79}$$

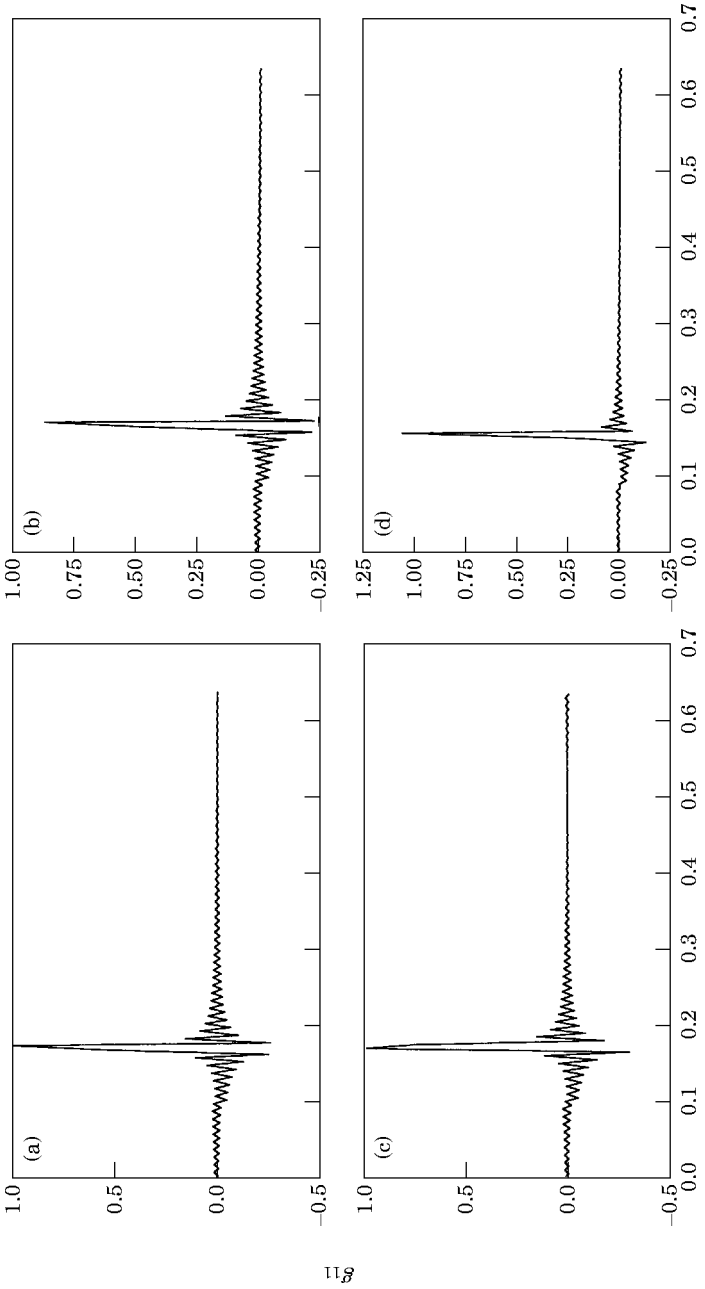

Figure 8. The normalized fundamental solution component g_{11} versus time t. (a) The homogeneous and (b) the heterogeneous deposit by the present method; (c) single-layered and (d) double-layered medium by program "hspec 91".

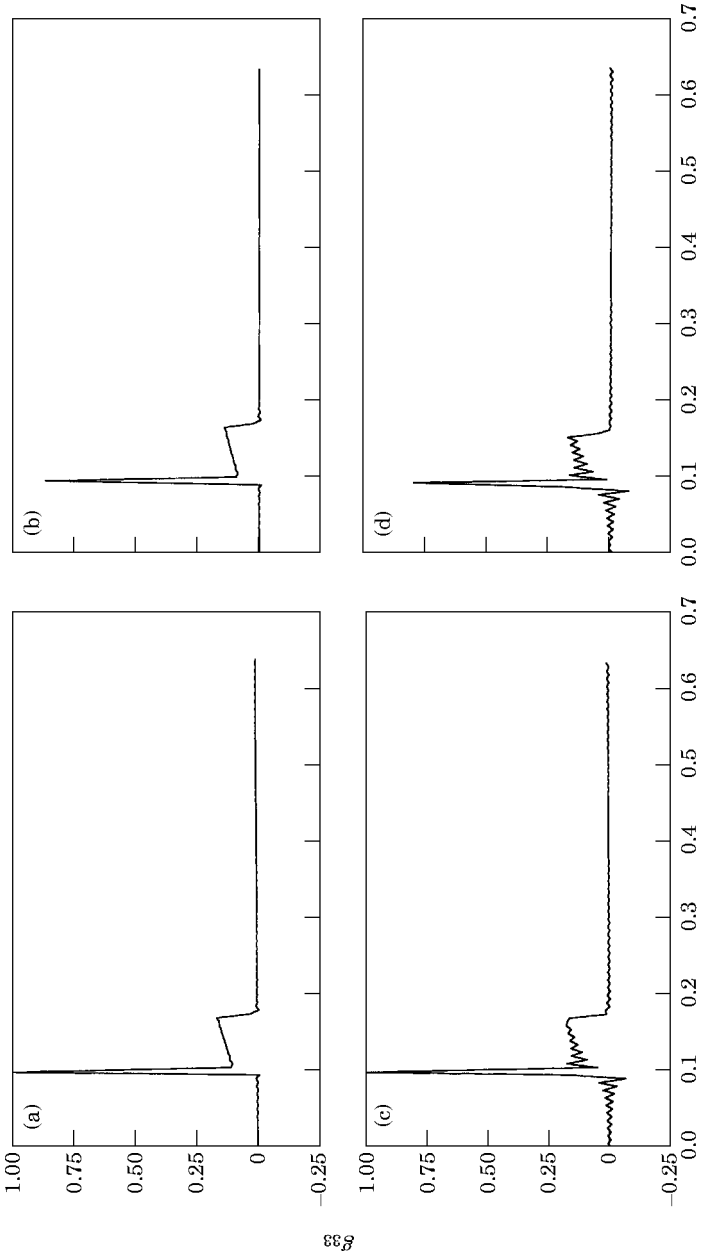

Figure 9. The normalized fundamental solution component g_{33} versus time t. (a) The homogeneous and (b) the heterogeneous deposit by the present method; (c) single-layered and (d) double-layered medium by program "hspec 91".

We note in passing that velocity and acceleration signals can be obtained by multiplying the displacement signal in the frequency domain prior to inversion by $-i\omega$ and ω^2, respectively. Also, viscoelastic material behavior is introduced by employing the Kelvin model and assigning the following values to the parameters appearing in equation (70):

$$q_0 = \mu_0, \qquad \omega q_1 = q_0 / 4Q^2 \qquad \text{and} \qquad p_1 = 0, \tag{80}$$

where the dimensionless quality factor $Q = 200$ for rock materials.

Concurrently plotted in Figures 8 and 9 are results obtained from the commercial software program "hspec 91" [39], which computes transient signals due to buried dislocation sources in a multi-layered viscoelastic medium, using the method developed in Wang and Herrmann [22]. We invoke the option for determining the transient Green function due to a point impulse (which corresponds to a fixed seismic moment of 10^{20} dyn-cm) for an arbitrary source–receiver configuration inside viscoelastic layers sandwiched between two homogeneous elastic half-spaces. Furthermore, the program employs cylindrical co-ordinates, and the point force at the source can be oriented along horizontal and vertical directions. Values for the material parameters in the case of a single intermediate layer are given by equation (72). In order to approximate the heterogeneous deposit, we employ a two-layer configuration, and material parameter values are interpolated using equations (66–68); i.e., the top layer containing the source has wavespeeds of $c_p = 5551$ m/s and $c_s = 3205$ m/s, while the lower layer containing the receiver has $c_p = 5963$ m/s and $c_s = 3443$ m/s. Also, the density and quality factor are unchanged and are equal to $\rho = 2100$ kg/m^3 and $Q = 200$, respectively.

All results have been normalized by dividing by the peak value encountered for the relevant homogeneous case (i.e., by $g_{11} = 0{\cdot}657 \times 10^{-9}$ and $g_{33} = 0{\cdot}109 \times 10^{-8}$ for the present method and by $g_{11} = 0{\cdot}946 \times 10^{-9}$ and $g_{33} = 0{\cdot}472 \times 10^{-9}$ for program "hspec91", all in m^{-2}) during the time interval of interest. In particular, the vertical displacement signal shows a sharp jump upon arrival of the P-wave at a time t_{p0} and a quiescent state is achieved past the arrival of the S-wave at time t_{s0}. As far as the horizontal displacement signal is concerned, we observe a predominantly SH wave-type situation, since the sharp jump in the signal occurs upon arrival of the S-wave at time t_{s0}. In both cases, the presence of heterogeneity has two basic effects; namely, the signal amplitude is reduced since the layer is stiffer in the direction of propagation (the horizontal component for the two layer configuration has about the same amplitude but looks less intense), and the first signal arrival is early by one to two time steps Δt, again for the same reason. The amount of heterogeneity is not very pronounced so that the basic transient signal shapes change only slightly. Finally, we observe that: (i) both programs yield essentially identical results for the homogeneous, single-layer case, which implies that the present methodology is equivalent to that of reference [22] when the material parameters are constant; and (ii) the double-layer representation of the continuously heterogeneous deposit examined herein is acceptable, since both programs again yield similar results.

8. CONCLUSIONS

This work presents a methodology for computing wavefields produced by a point source in special class of heterogeneous materials. More specifically, we consider an unbounded three-dimensional medium with elastic parameters that depend on a single co-ordinate (taken to be the depth for convenience) which satisfy the following conditions: a Poisson ratio of 0·25, a shear modulus which varies quadratically in the depth co-ordinate, and constant, linear or quadratic density profiles. The first two constraints are dictated by the algebraic transformation procedure which is applied to both displacement and forcing

function vectors, while the last one is a consequence of the matrix differential equation formulation and subsequent series solution of the doubly Fourier transformed equations of motion. Since we focus on time harmonic waves, viscoelastic material behavior can be captured through use of the correspondence principle. The final step in the solution procedure involves inverse transformation from the wavenumber domain back to the (x, y) co-ordinate space using the double FFT. Also, standard Fourier synthesis is used for capturing the transient response. Finally, a few numerical examples serve to validate the methodology and to present results for a material with linearly varying (in the depth co-ordinate) wavespeeds.

The present methodology combines the simplicity of an algebraic transformation procedure with the efficiency of a first order matrix differential equation solution. Furthermore, the methodology is easily adapted to model axisymmetric and plane strain cases with an added simplification; namely, a single Fourier transform in lieu of the double one employed herein. A drawback is that a numerical inverse Fourier transformation is required which, however, is easily accomplished given the present status of multi-dimensional FFT algorithms. As such, the methodology is a useful addition to the relatively few existing methods for simulating wavefields in continuously inhomogeneous media. The constraints on the elastic moduli cannot, of course, be lifted, but the method can become more general by introducing a traction-free horizontal surface to model a half-space and by superposition of point sources to produce the effect of a finite-size source. Finally, the Green function recovered herein can be used as a kernel function within the context of integral equation methods for solving wave scattering types of problems.

ACKNOWLEDGMENTS

We wish to thank Mrs M. Vafeiadou for typing the manuscript and Dr D. Raptakis for his help with the program "hspec91".

REFERENCES

1. W. M. Ewing, W. S. Jardetzky and F. Press 1957 *Elastic Waves in Layered Media*, New York: McGraw-Hill.
2. A. Ben Menachem and S. J. Singh 1981 *Seismic Waves and Sources*. New York: Springer-Verlag.
3. L. M. Brekhovskikh and R. Beyer 1980 *Waves in Layered Media*. New York: Academic Press.
4. W. C. Chew 1990 *Waves and Fields in Inhomogeneous Media*. New York: Van Nostrand-Reinhold.
5. E. Bahar 1967 *Journal of Mathematical Physics* **8**, 1735–1746. Generalized WKB method with applications to problems of propagation in nonhomogeneous media.
6. Y. B. Liu and R. S. Wu 1994 *Bulletin of the Seismological Society of America* **84**, 1154–1168. A comparison between phase screen, finite difference and eigenfunction expansion calculations for scalar waves in inhomogeneous media.
7. Y. Hisada 1994 *Bulletin of the Seismological Society of America* **84**, 1456–1472. An efficient method for computing Green's functions for layered half-space with sources and receivers at close depths.
8. J. Zhu, A. H. Shah and S. K. Datta 1994 *Journal of Engineering Mechanics*, *American Society of Civil Engineers* **121**, 26–36. Modal representation of two-dimensional elastodynamic Green's function.
9. C. L. Pekeris 1946 *Journal of the Acoustical Society of America* **18**, 295–315. Theory of propagation of sound in a half-space of variable sound velocity under conditions of formation of a sound zone.
10. Y. L. Li, C. H. Liu and S. J. Franke 1990 *Journal of the Acoustical Society of America* **87**,

2285–2291. Three-dimensional Green's function for wave propagation in a linearly inhomogeneous medium—the exact analytic solution.
11. D. M. Pai 1991 *Wave Motion* **13**, 205–209. Wave propagation in inhomogeneous media: a planewave layer interaction method.
12. B. G. Mikhailenko 1985 *Journal of Geophysics* **58**, 101–124. Numerical experiments in seismic investigations.
13. B. G. Mikhailenko 1984 *Geophysics Journal of the Royal Astronomical Society* **79**, 963–986. Synthetic seismograms for complex three dimensional geometries using an analytical–numerical technique.
14. J. Gazdag 1973 *Journal of Computer Physics* **13**, 100–113. Numerical convective schemes based on accurate computation of space derivatives.
15. H. K. Acharya 1971 *Journal of the Acoustical Society of America* **50**, 172–175. Field due to a point source in an inhomogeneous elastic medium.
16. P. Ugincius 1972 *Journal of the Acoustical Society of America* **51**, 1759–1763. Ray acoustics and Fermat's principle in a moving inhomogeneous medium.
17. J. F. Hook 1961 *Journal of the Acoustical Society of America* **33**, 302–313. Separation of the vector wave equation of elasticity for certain types of inhomogeneous, isotropic media.
18. R. C. Alverson, F. C. Gair and J. E. Hook 1963. *Bulletin of the Seismological Society of America* **53**, 1023–1030. Uncoupled equations of motion in nonhomogeneous elastic media.
19. R. N. Gupta 1966 *Bulletin of the Seismological Society of America* **56**, 511–526. Reflection of elastic waves from a linear transition layer.
20. R. G. Payton 1966 *Quarterly Journal of Mechanics and Applied Mathematics* **19**, 83–91. Elastic wave propagation in a nonhomogeneous rod.
21. F. C. Karal and J. B. Keller 1959 *Journal of the Acoustical Society of America* **31**, 694–705. Elastic wave propagation in homogeneous and inhomogeneous media.
22. C. Y. Wang and R. B. Herrmann 1980 *Bulletin of the Seismological Society of America* **70**, 1015–1036. A numerical study P-, SV-, and SH-wave generation in a plane layered medium.
23. N. A. Haskell 1964 *Bulletin of the Seismological Society of America* **54**, 337–393. Radiation pattern of surface waves from point sources in multi-layered medium.
24. L. Cagniard 1962 *Reflection and Refraction of Progressive Seismic Waves* (English translation). New York: McGraw-Hill.
25. J. A. Hudson 1969 *Geophysics Journal* **18**, 353–370. A quantitative evaluation of seismic signals at teleseismic distances—II. Body waves and surface waves from an extended source.
26. A. Umek and A. Strukelj 1987 *Ground Motion and Engineering Seismology* (A. S. Cakmak, editor) **44**, 339–345. Amsterdam: Elsevier. Green's function for layered halfspace.
27. R. J. Apsel and J. E. Luco 1983 *Bulletin of the Seismological Society of America* **73**, 931–951. On the Green's functions for layered half-space, part II.
28. W. Thomson 1950 *Journal of Applied Physics* **21**, 89–93. Transmission of elastic waves through a stratified solid medium.
29. E. Kausel and J. M. Roesset 1981 *Bulletin of the Seismological Society of America* **71**, 1743–1761. Stiffness matrices for layered soil.
30. M. A. Bravo, F. Sanchez-Sesma and F. Chavez-Garcia 1988 *Bulletin of the Seismological Society of America* **78**, 436–450. Ground motion on stratified alluvial deposits for incident SH waves.
31. G. D. Manolis and R. P. Shaw 1996 *Wave Motion* **24**, 59–83. Green's function for the vector wave equation in a mildly heterogeneous continuum.
32. G. D. Manolis and R. P. Shaw 1997 *Soil Dynamics and Earthquake Engineering* **16**, 81–94. Fundamental solutions to Helmholtz's equation for inhomogeneous media by a first-order differential equation system.
33. J. D. Achenbach 1973 *Wave Propagation in Elastic Solids*. Amsterdam: North Holland.
34. A. Erdelyi (editor) 1954 *Tables of Integral Transforms*. New York: McGraw-Hill.
35. M. Braun 1975 *Differential Equations and their Applications*. Berlin: Springer-Verlag.
36. V. S. Vladimirov 1984 *Equations of Mathematical Physics*. Moscow: MIR.
37. W. H. Press, B. P. Flannery, S. A. Teukolsky and W. T. Vetterling 1989 *Numerical Recipes* (*Fortran Version*), Cambridge: Cambridge University Press.
38. R. M. Christiansen 1982 *Theory of Viscoelasticity*: *an Introduction*. San Diego: Academic Press.
39. R. B. Herrmann 1993 *Computer Programs in Seismology* **6**, St. Louis: St. Louis University Publication.